TESCAN

A unique combination of Plasma FIB and field-free UHR SEM for the widest range of multiscale materials characterization applications

1 mm cross-section through a Li-ion battery electrode

TESCAN AMBER X

- ✓ High throughput, large area FIB milling up to 1 mm
- ✓ Ga-free microsample preparation
- ✓ Ultra-high resolution, field-free FE-SEM imaging and analysis
- ✓ In-column SE and BSE detection
- ✓ Spot optimization for high-throughput, multi-modal FIB-SEM tomography
- ✓ Superior field of view for easy navigation
- ✓ Essence™ easy-to-use, modular graphical user interface

For more information visit

www.tescan.com

ADVANCED ENERGY MATERIALS
www.advenergymat.de

Waste Recycling in Thermoelectric Materials

*Amin Bahrami, Gabi Schierning, and Kornelius Nielsch**

Thermoelectric (TE) technology enables the efficient conversion of waste heat generated in homes, transport, and industry into promptly accessible electrical energy. Such technology is thus finding increasing applications given the focus on alternative sources of energy. However, the synthesis of TE materials relies on costly and scarce elements, which are also environmentally damaging to extract. Moreover, spent TE modules lead to a waste of resources and cause severe pollution. To address these issues, many laboratory studies have explored the synthesis of TE materials using wastes and the recovery of scarce elements from spent modules, e.g., utilization of Si slurry as starting materials, development of biodegradable TE papers, and bacterial recovery and recycling of tellurium from spent TE modules. Yet, the outcomes of such work have not triggered sustainable industrial practices to the extent needed. This paper provides a systematic overview of the state of the art with a view to uncovering the opportunities and challenges for expanded application. Based on this overview, it explores a framework for synthesizing TE materials from waste sources with efficiencies comparable to those made from raw materials.

1. Introduction

The urgent need to reduce the world's dependence on fossil fuels has fueled research into, and the adoption of, renewable energy. Indeed, according to the US Energy Information Administration (EIA), US monthly electricity generation from renewable sources exceeded coal-fired generation for the first time in April 2019. This reflects long-term increases in renewable-energy generation and decreases in coal burning.[1] Although the EIA defines renewable energy in terms of utility-scale hydropower, wind, solar, geothermal, and biomass, there is a strong case for also including thermoelectricity in this category.

Solid-state thermoelectric generators (TEGs) convert heat (temperature gradient) to electrical energy using principles such as Seebeck, Peltier, and Thomson effects.[2] Such generators can be used to transform waste heat generated from power plants, factories, motor vehicles, computers, or even human bodies into electricity. TEGs are suitable for small applications because of their compatibility, simplicity, and scalability. For example, electricity can be generated from small heat sources and by taking advantage of small temperature differences for powering wristwatches or wearable devices such as miniaturized accelerometers or electroencephalography (EEG) devices.[3,4] However, low efficiency and high fabrication cost are the main disadvantages of TEGs which hinder their vast application in the market. Although many studies have explored the ways to increase the efficiency of TEGs in converting the thermal to electric energy, cost of TE materials synthesis and miniaturized TEGs fabrication has not been addressed widely.

TEGs require materials with high electrical conductivities and low thermal conductivities, as well as high thermopower (Seebeck coefficient, S) which in turn constrains the types of materials that can be used as a TE material. The direct conversion of thermal to electrical energy in response to a temperature gradient across a material can be calculated by using the following equation

$$\Delta V = -S\,\Delta T \tag{1}$$

where ΔV is the generated voltage, S is the Seebeck coefficient or thermopower, and ΔT is the temperature difference. The performance of a TE material is defined by the dimensionless figure of merit (zT), which relates the material properties to its conversion efficiency, in the following way

$$ZT = \frac{S^2\,\sigma\,T}{(\kappa_l + \kappa_e)} \tag{2}$$

where σ is the electrical conductivity, κ_l and κ_e are the lattice and electronic contributions to the thermal conductivity of TE material, respectively, and T is the absolute temperature. High $S^2\sigma$ (power factor, PF) and low thermal conductivity, $\kappa = \kappa_l + \kappa_e$, lead to better performance. In practice, however, the mutual dependence between these material properties makes an optimization of zT difficult.

For many decades since the 1950s, when research and development of bulk homogenous materials for TE applications started to increase, research and development efforts focused on elements derived from raw materials for synthesizing TE materials. The compounds synthesized from raw elements such as

Dr. A. Bahrami, Dr. G. Schierning, Prof. K. Nielsch
Leibniz Institut für Festkörper- und Werkstoffforschung Dresden e.V.
Institut für Metallische Werkstoffe
Helmholtzstr. 20, Dresden 01069, Germany
E-mail: k.nielsch@ifw-dresden.de

The ORCID identification number(s) for the author(s) of this article can be found under https://doi.org/10.1002/aenm.201904159.

DOI: 10.1002/aenm.201904159

Zn, Sb, Bi, Te, etc., possessed the requisite attributes to ensure the optimal performance of TE materials in some niche applications. However, as the demand for TEGs increased from the 1990s onward, the reliance on raw materials started posing difficulties. Many of the elements used in TE materials are either found in extremely low concentrations in minerals or are mixed up with other elements with similar physical and chemical properties: this makes the extraction procedure difficult and costly.[5] Moreover, both the mining for raw materials and the waste consisting of spent TE modules lead to severe environmental consequences.[6,7] Given the growing interest in more sustainable sources of energy, the demand for TE materials in technologies such as climate control seat (CCS) in cars passenger seats, power generators, thermal energy sensors and radioisotope TEGs for interplanetary spacecraft will grow. As a consequence, the amount of waste TE materials will increase significantly in the forthcoming years,[8] and the reliance on raw materials will only exacerbate the costs and environmental problems.

An alternative to extracting elements from raw materials is to extract such elements from waste or recycled material. Indeed, the increasing number of solar panels harvesting via photovoltaic cells and consumer electronics, which are discarded after they expire, is a potential source of Si-containing wastes. In addition, many agricultural wastes also contain silica (SiO_2).[9,10] The recycling of scarce elements from spent TE materials or using waste from either industrial or agricultural origins in order to synthesis new TE compounds could reduce the need for raw materials, thereby minimizing costs, energy, and the human impact on the environment.

The first time a waste material was used in the synthesis of a TE material was in the 1990s (rice husk to synthesize magnesium disilicide; Mg_2Si).[11] Unfortunately, neither the use of waste materials in the synthesis of TE materials nor the recycling of TE materials are common at the industrial scale: almost all recycling or recovery technologies and processes remain at the laboratory level. This is because of two main reasons:

i) Until recently, there were no strict regulations that prevented the disposal of industrial wastes such as discarded Si sludge and metallurgical slags in landfills or the incineration of agricultural wastes such as rice husk.
ii) Crucial gaps remain in the knowledge about the properties of different waste materials and about recycling of different elements from the TE material, which leads to a lack of confidence among customers.

In spite of the numerous research and review articles on advent of new TE materials and development of TE devices with high efficiency,[12–20] up to now, no review paper with an ample and varied references source has been published analyzing and discussing waste recycling issue in the field of TE materials. In addition, scarce elements recovery from EoL-TE modules is a state-of-the-art topic because many TE modules already reached to the substantial production volume and their recycling should be taken into account. It is worth noting that scarce elements recovery from EoL devices is focused mainly on waste electrical and electronic equipment (WEEE) such as computers, TV sets, fridges, and cell phones.[21–23] In this article (**Figure 1**), we provide an overview of the use of waste materials in the fabrication of TE materials and recycling of spent TE modules. We first review studies on the use of waste materials such as rice husk, cast-iron scrap chips, recycled carbon fiber sheets, etc., in the synthesis of TE materials. Specifically, we focus on the methods of preparing different wastes before their use in synthesizing TE materials. We then review studies on the recycling of TE modules. In particular, we compare the thermoelectric performance of recycled materials with the same composition

Amin Bahrami is an Alexander von Humboldt research fellow at Leibniz Institut für Festkörper- und Werkstoffforschung Dresden (IFW), Germany. In 2016 he received his Ph.D. in materials science from CINVESTAV (México). He worked as a postdoctoral researcher at Universidad Nacional Autónoma de México (UNAM) until end of 2018. His present research activity is focused on synthesis new thermoelectric materials.

Gabi Schierning is head of the department thermoelectric materials and devices at Leibniz Institut für Festkörper- und Werkstoffforschung Dresden (IFW), Germany. Before that she was a group leader of an independent young researcher group at the University of Duisburg-Essen, Germany. She received her Ph.D. degree in materials science from the University of Erlangen-Nuremberg, Germany, in 2005.

Kornelius Nielsch has studied physics at the University Duisburg and received the master's thesis from Lund University in 1997. For Ph.D. he joined the Goesele group at the Max-Planck-Institute Halle. In 2002/2003, he worked as a postdoc at MIT. Subsequently, he led a young investigator group at Max-Planck-Institute Halle. In 2006, the Hamburg University has appointed him as W2 professor. In 2015, he became the director of the Institute of Metallic Materials at IFW Dresden.

Figure 1. A schematic showing the synthesis of TE materials using waste materials and wastes recycling in thermoelectric materials. Some industrial and agricultural wastes can be considered as potential starting materials for the synthesis of TE materials.

obtained from raw materials to evaluate the feasibility of using wastes to synthesize TE materials. Therefore, the aim of this paper is to review studies of the scientific, environmental and economic impact of reuse and recycling in TE materials, to provide a summary of the current knowledge and point out areas for further research.

2. Use of Wastes in the Synthesis of TE Materials

Since wastes were first used in the synthesis of TE materials, most work has focused on synthesizing Mg_2Si and Bi_2Te_3 from different agricultural and industrial waste sources, probably because of their simple chemical composition and widespread use in thermoelectric devices. However, some other TE materials such as SiC and $FeSi_2$ can also be obtained from waste sources. In the following subsections, we review previous work on synthesizing TE materials from such wastes.

2.1. Mg_2Si-Based TE Materials from Wastes

Mg_2Si was introduced as a promising and advanced TE material in the early 1960s, with an operating-temperature range of 500–800 K.[24–26] Mg and Si are both nontoxic elements that are abundant in the Earth's crust, which makes Mg_2Si more environmentally friendly than $CoSb_3$ and PbTe, for example, which have the same operating-temperature range. However, in addition to improvements in thermoelectric properties,[27] it is also important to reduce the cost of the raw materials and manufacturing processes to increase the cost performance measure of a device.[28] This consideration prompted investigations of the potential for various types of waste materials to synthesize Mg_2Si and other TE materials.

2.1.1. Rice Husk

Rice husk is a dramatic source of pollution and has adverse effects on ecosystems: its hard surface, small bulk density, and high silicon content mean that it cannot be easily decomposed by bacteria. The emission of rice husk and rice husk ash into the ecosystem has provoked huge criticisms and complaints, mainly associated with its persistent, carcinogenic, and bioaccumulative effects, resulting in silicosis syndrome, fatigue, shortness of breath, loss of appetite, and respiratory failure.[9,29] The world rice harvest, according to Food and Agriculture Organization of United Nations (FAO) rice market monitor (RMM) in 2018 is estimated in 769.9 million tons. Considering that 20% of the grain is husk, and 20% of the husk after combustion is converted into ash, a total of 30.8 million tons of ash can be obtained each year.[30] There has been considerable previous work on rice-husk valorization through physical and chemical treatments. The initial steps for extracting any Si-based compound out of rice husk are incineration and acid/base washing, which get rid of organics such as hemicellulose, cellulose, lignin and etc. To date, different Si-based materials, such as pure Si, Mg_2Si, Si_3N_4, SiO_2,

SiC, and active carbon, have been synthesized, with established applications in electronics, absorbents, rubber fillers, insulators, and other areas.[31–33] The use of rice husk to synthesize Si-based ceramics and TE materials could thus help cut costs while also contributing to the disposal of potentially hazardous materials.

Bose pioneered the use of rice husk for the synthesis of Mg_2Si as a TE material in 1992–1993.[11,34] He used two different ways to obtain Mg_2Si from rice husk ash (RHA).[34] In the first method, SiO_2 obtained from rice husk was first mixed with pure magnesium powder in an appropriate quantity. The mixture was then packed in a metallic crucible and covered with salts like NaCl with a low melting point. Finally, the reaction was initiated using an ignited Mg ribbon or current passing through a filament inserted in the mixture. This method of synthesis is well described by Acharya et al.[35] In the second method, powdered solar-grade Si from rice husk and pure magnesium were mixed and heated up to 773 K in a furnace for 24 h under H_2 atmosphere to synthesize Mg_2Si.

Following synthesis, κ was measured for different Mg_2Si powder compacts with different particle sizes. For powders prepared using the crucible ignition method, the measurements yielded no definite relation between the particle size and the effective κ. This does not agree with the fact that TE material with higher particle size has always higher κ compared to the material with lower particle size.[36] This inconsistency was explained by the presence of unwanted phases such as MgO in the powder compact. However, for the powders obtained from direct reaction of Si with Mg by alloying, κ decreased with decreasing particle size as expected.[34] Therefore, the second method which is the reaction of pure Mg and solar grade Si from rice husk, provided Mg_2Si powders from with higher purity than that of the first method. This can be attributed to the fact that no oxide phases were incorporated in the synthesis of Mg_2Si from rice husk.

In a subsequent study done by Bose et al., the obtained powders from the second route were compacted in a furnace under an argon atmosphere at 823 K for 24 h.[11] The samples showed $S = 565\ \mu V\ K^{-1}$, $\rho = 35\ \Omega$ Cm, and $\kappa = 2.6\ W\ K^{-1}\ m^{-1}$ at 303 K. The differential thermal analyses (DTA) record did not reveal any phase change or other reaction when the sample was heated from 300 to ≈1253 K at a uniform heating rate. Also, it was observed that the smaller the grain size, the lower σ and S. $zT = 1 \times 10^{-4}$ was obtained for the sample with large grain size at room temperature.

To conclude, the results of these two studies suggest that the thermoelectric performance of Mg_2Si synthesized from rice husk is not as promising as that obtained from other sources (see below) because impurities from the rice husk are transferred to the Mg_2Si (see **Table 1**).

2.1.2. Silicon Sludge and Magnesium-Alloy Scrap

Both Si and Mg waste generated from various manufacturing processes is a potential starting point for the synthesis of TE materials. Solar-grade silicon (SOG) is the material of choice in the solar market because it enables relatively efficient conversion of solar energy into electricity.[37,38] 60% of the total manufacturing cost of a Si-based photovoltaic solar cell is for fabrication of crystalline Si (including both large-grain polycrystalline and single-crystalline materials). During the cutting of Si ingots with wire, 40% of Si is wasted (kerf), and there is an annual loss of 2 billion USD dollars just during the cutting of Si wafers.[39,40] Mg-alloy scrap originates from end-of-life vehicles or chips produced during the manufacturing processes. The extraction of Mg ore is extremely expensive because of high energy consumption, so the recycling of Mg alloy will undoubtedly become important.[41,42]

Two studies in Japan used silicon sludge and magnesium-alloy scrap for synthesizing Mg_2Si.[43,44] In the first study, Akasada et al.[43] used silicon sludge and pure Mg to synthesize Mg_2Si powder. First, the Si source (100% reused Si from sludge and a 50:50 mixture of reused Si and solar grade Si) was mixed with Mg powder and melted in a presynthesis process. Then, 2 at% of Bi or 5 at% of Ag was added to the composition as a dopant. Glow discharge mass spectrometry (GDMS) analyses revealed that the sample prepared from 100% reused Si contained Sb and As, which are common n-type dopants used in the fabrication of the n-type Silicon substrates. TE performance characterization showed that the undoped sample made of the reused-Si had a smaller S and a higher σ than the sample from the solar-grade Si source. The PFs of undoped samples from the reused-Si source were comparable to those from the 50:50 mixture of reused Si and solar-grade Si source. The zT values of Mg_2Si samples synthesized from Si sludge were insignificantly lower than the zT values of the samples synthesized from the mixture Si source (see **Figure 2**a,b). These results suggested that waste Si can be an effective substitute for solar grade Si.

In the second study, Honda et al. used waste Mg alloys as a source of Mg together with a reused Si source.[44] They tried various combinations of waste and pure materials to find the combination with the highest zT value. The results revealed that the zT values for the samples fabricated from waste Si and recycled Mg alloys were about 0.6 at 860 K, whereas there was no significant difference between the zT values of samples synthesized from 100% solar-grade Si and 100% reused Si sources (Figure 2). The authors concluded that a combination of reused Si and Mg alloy could be used to fabricate material that is capable of significant power generation of ≈29 mW at 500 K.

In a separate study, Isoda et al.[45] used three different sources of Si to synthesize Mg_2Si using a direct liquid-solid phase reaction: 1) metal-grade Si (99% pure), 2) solar-grade Si (99.9999% pure), and 3) waste-sludge Si that contained surfactants, silicon carbide particles, and metallic fragments. The sludge Si was washed before use to get rid of all organic compounds. The x-ray diffraction (XRD) pattern of the sludge Si (**Figure 3**a) revealed the presence of impurities such as silica and carbon, which indicated that unwanted phases such as MgO and SiC also form along with Mg_2Si. Chemical analysis of the sintered Sb-doped Mg_2Si samples (Figure 3b) revealed that the amount of Fe and Al impurities were much higher than other elements. This could be attributed to the pulverization of the starting materials by iron-stamp mills and alumina mortars. Metal-grade Si was found to be the source with the highest amount of impurities such as B, Fe, Al, Ni, Ca, Cu, Ti, Cr, Mn, V, and Zn.

The PF values increased uniformly with increasing temperature up to 600 K for the samples prepared from metallic

Table 1. Summary of properties of Mg_2Si-based TE materials obtained from waste sources and pure starting materials, and doped by different dopants.

Type	Chemical composition	Waste source	σ [Ω^{-1} cm^{-1}]	S [μV K^{-1}]	PF [W m^{-1} K^{-1}]	κ [W m^{-1} K^{-1}]	zT max.	Temp. [K]	Ref.
n	Mg_2Si	Rice husk	2.22	−618.4	2.7×10^{-2}	2.34	117.6×10^{-4} [a]	344	[11]
	Mg_2Si	Sludge Si	373.09	−219.66	1.45	3.34	0.43	843	[43]
	Mg_2Si	SG [b] Si	244.97	−269.67	1.43	3.07	0.47	843	
	Mg_2Si–2% Bi	Sludge Si	626.15	−205.07	1.98	3.9	0.51	860	
	Mg_2Si–2% Bi	SG Si	568.22	−188.04	1.58	2.9	0.54	847	
	Mg_2Si	Sludge Si/PM [c]	355.77	−240.78	1.77	2.98	0.61	860	[44]
	Mg_2Si	SG Si/PM	505.28	−224.61	2.19	3.66	0.60	860	
	Mg_2Si–1 at% Al	Sludge Si/PM	527.93	−206.52	1.94	3.34	0.59	860	
	Mg_2Si–2 at% Al	Sludge Si/PM	505.28	−209.38	1.91	3.63	0.52	860	
	Mg_2Si–1 at% Bi	Sludge Si/PM	611.03	−195.10	2.0	3.02	0.66	860	
	Mg_2Si–2 at% Bi	Sludge Si/PM	728.19	−197.96	2.45	2.89	0.85	860	
	Mg_2Si–5.8 at% Al	SG Si/AZ91D scrap	505.28	−208.43	1.89	3.37	0.55	860	
	Mg_2Si–3.9 at% Al	SG Si/AM60B scrap	505.28	−201.77	1.77	3.69	0.48	860	
	Mg_2Si–5.8 at% Al	SG Si/AZ91D scrap	497.50	−210.33	1.89	3.49	0.54	860	
	Mg_2Si–3.9 at% Al	SG Si/AM60B scrap	551.60	−203.67	1.96	3.12	0.63	860	
	$Mg_2Si_{0.992}Sb_{0.008}$	Sludge Si	869.4	−167.39	2.1	3.66	0.57	855	[45]
	$Mg_2Si_{0.992}Sb_{0.008}$	SG Si	557.7	−208.90	2.04	3.50	0.58	855	
	$Mg_2Si_{0.992}Sb_{0.008}$	MG [d] Si	517.9	−210.46	1.96	3.49	0.56	855	
	$Mg_2Si_{0.992}Sb_{0.008}$	Sludge Si	256.64	−163.37	1.46	4.45	0.33	843	[47]
	$Mg_{1.85}Si_{0.992}Sb_{0.008}$	Sludge Si	141.01	−238.21	0.93	3.35	0.28	843	
	$Mg_{1.85}Si_{0.984}Sb_{0.016}$	Sludge Si	168.30	−226.02	1.18	3.39	0.35	843	
	$Mg_{1.85}Si_{0.96}Sb_{0.04}$	Sludge Si	249.75	−197.20	2.02	3.06	0.66	843	
	$Mg_2Si_{0.55}Ge_{0.05}Sn_{0.4}$/5%Bi	Si kerf	1011.4	−192.82	2.93	2.87	1.02	770	[40]
	$Mg_2Si_{0.55}Ge_{0.05}Sn_{0.4}$/5%Sb	Si kerf	1094	−191.09	3.17	3.26	0.97	785	
	$Mg_2Si_{0.4}Sn_{0.6}$/5%Bi	Si kerf	816.56	−231.3	3.39	2.60	1.31	774	
p	Mg_2Si–5% Ag	Sludge Si	78.92	196.35	6.0	–	–	862	[43]
	Mg_2Si–5% Ag	SG Si	89.83	225.27	6.38	–	–	873	

[a] zT is calculated based on the temperature range available for κ data in ref. [11] and is not the maximum value; [b] Solar grade silicon; [c] Pure Mg; [d] Metal grade silicon.

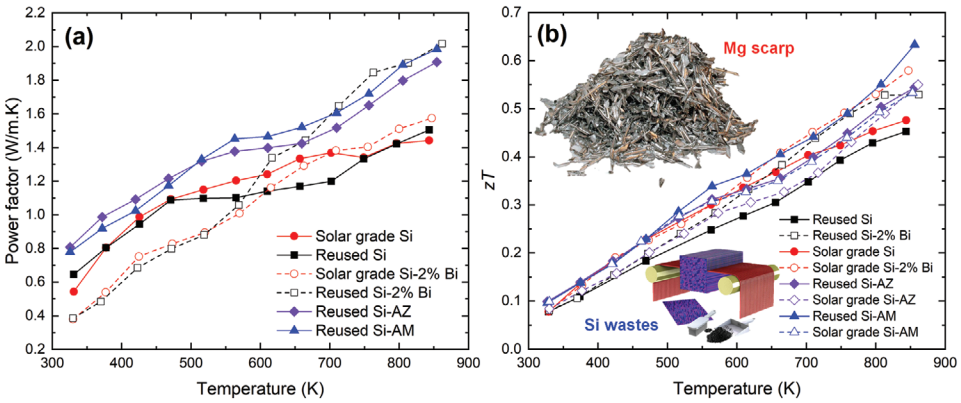

Figure 2. a) PF and b) zT of the sintered Mg_2Si-based compounds synthesized using different silicon and magnesium sources as a function of temperature.[43,44] AZ: AZ91D magnesium alloy; AM: AM60B magnesium alloy. Both filled and hollow circles are for a 50:50 mixture of reused Si and solar grade Si.

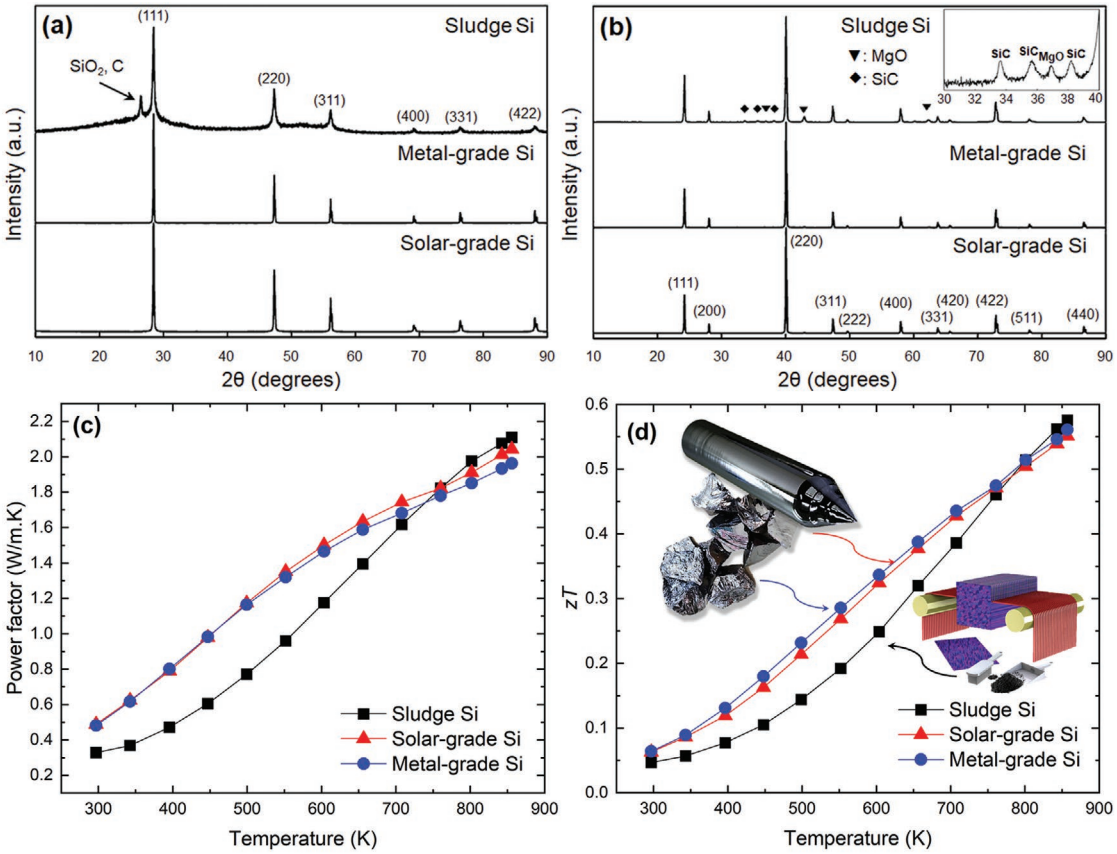

Figure 3. XRD pattern of a) silicon source powders and b) the sintered Sb-doped Mg_2Si samples produced using different silicon sources. Inset in (b) shows magnified XRD patterns for the sintered Sb-doped Mg_2Si sample produced using sludge silicon. c) PF and d) zT of the sintered $Mg_2Si_{0.992}Sb_{0.008}$ samples synthesized using different silicon sources as a function of temperature. Reproduced with permission.[45] Copyright 2016, Springer.

and solar grade Si (Figure 3c). Above this temperature, the PF decreased slightly. The maximum PF value of 1.5 W m^{-1} K^{-1} at 600 K was obtained for the sample prepared from solar-grade Si. At lower temperatures, the PF of sample synthesized from sludge Si was significantly lower than those from other sources. However, its PF increased at higher temperatures, reaching 2.12 W m^{-1} K^{-1} at 860 K. zT increased monotonically with increasing temperature (Figure 3d), reaching a maximum value of 0.56 at 855 K, 0.55 at 858 K, and 0.57 at 855 K for the samples prepared from metal-grade Si, solar-grade Si, and sludge Si, respectively. The maximum zT values for all three samples were almost the same and in good agreement with that of $Mg_2Si_{0.98}Sb_{0.02}$ as reported by Tani et al.[46] The observed behavior of samples obtained from sludge Si could be attributed to two facts: i) higher carrier concentration resulting from the excess Mg content, and ii) the reduction of κ_l due to the fine grain sizes. However, it should be noticed that the zT values of Mg_2Si obtained from solar and metal grade Si is higher than that of obtained from sludge Si in temperature less than 700 K. These results suggested that a low-purity Si source was adequate and that the production of Mg_2Si TE materials for high temperatures applications (above 700 K) is an effective means for recycling sludge Si.

Kitagawa et al.[47] used sludge Si as a Si source together with pure Mg and Sb as donor dopants to synthesis Mg_2Si powders. They used washed and unwashed sludge Si in order to determine how the impurities in the sludge affect the formation of single Mg_2Si phase or impurities. In the case of the washed sludge Si, a water-based agent was used before drying at 373 K for 3 h in air. The XRD pattern of the final phases (**Figure 4**) revealed a strong peak of Mg in all the samples synthesis using unwashed sludge Si. This unwanted metallic Mg phase could be reduced by decreasing the Mg content from 2 to 1.6, but it was not possible to completely eliminate it. Further, an MgO phase that originated from the SiO_2 in the sludge Si was also detected. The presence of Mg phase could be significantly suppressed by using washed sludge Si, although a small amount of an MgO phase still remained.

Kitagawa et al. reported that the carrier concentration of Mg_2Si synthesized from washed sludge Si could be tuned in the range of 10^{25} to 10^{26} m^{-3} by Sb doping.[47] The existence of metallic Mg in $Mg_2Si_{0.992}Sb_{0.008}$ caused a significant reduction of one order of magnitude in the carrier concentration as compared to that of $Mg_{1.85}Si_{0.992}Sb_{0.008}$. The results obtained for the PF were in complete accordance with the carrier concentration in each sample: the maximum PF of 2.02 W m^{-1} K^{-1} was found for the $Mg_{1.85}Si_{0.96}Sb_{0.04}$ sample at 843 K. The highest zT value of 0.66 was obtained for $Mg_{1.85}Si_{0.96}Sb_{0.04}$ at 843 K (Figure 4d). This value is slightly higher than the zT values reported by Tani et al.[46] (0.56 at 862 K for Mg_2Si: Sb = 1:0.02)

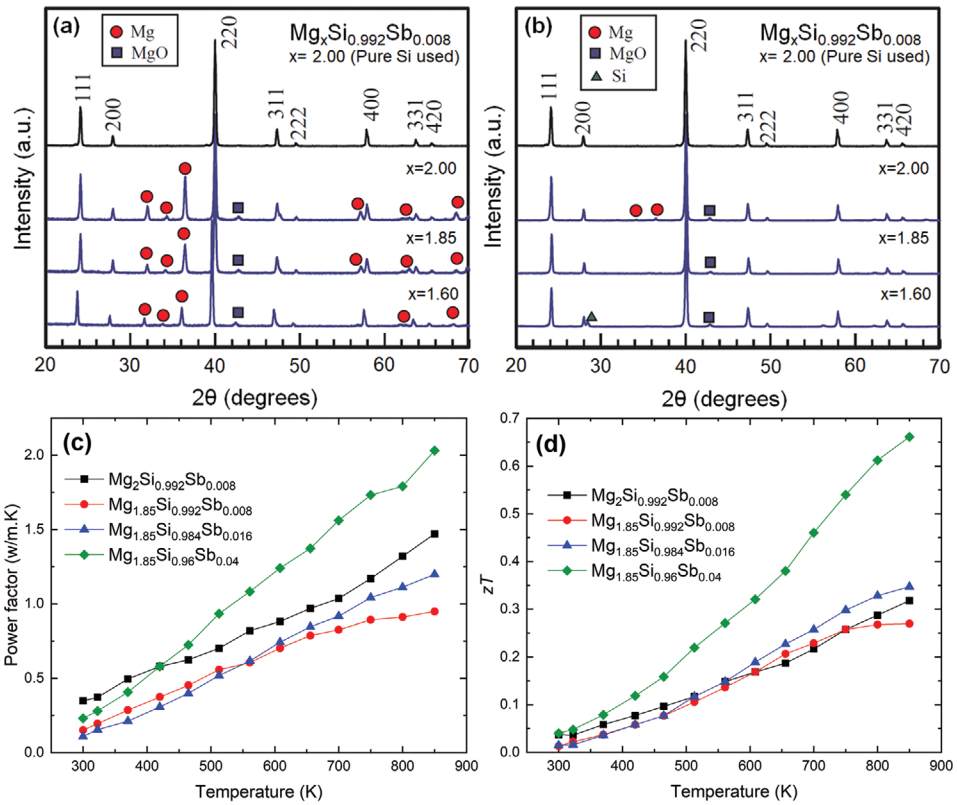

Figure 4. XRD patterns of $Mg_xSi_{0.992}Sb_{0.008}$ powders synthesized from a) unwashed sludge Si and b) washed sludge Si. The presence of Mg in the XRD patterns of powders derived from unwashed sludge Si indicates that the effect of washing of sludge Si on the phase constitution is drastic. The organic carbon and other impurities contained in the unwashed sludge Si also significantly affect the solid–liquid reaction. c) PF and d) zT of $Mg_2Si_{0.992}Sb_{0.008}$ and $Mg_{1.85}Si_{1-y}Sb_y$ ($y = 0.008$–0.04) prepared from washed sludge Si as a function of temperature. Reproduced with permission.[47] Copyright 2018, Elsevier.

and Ioannou et al.[48] (0.46 at 810 K for $Mg_2Si_{0.99}Sb_{0.01}$) for Sb-doped Mg_2Si TE materials with similar carrier concentrations that were obtained from pure Si.

Recently, Mesaritis et al.[40,49] processed slurry waste from cutting Si wafers to obtain powders with high Si concentration for the synthesis of $Mg_2Si_{1-x-y}Sn_xGe_y$-based TE materials using a modified three-step method.[50] Since the slurry obtained from cutting Si wafers contains Si, SiC, wire metal, glue, and polyethylene glycol, the group attempted to remove all unwanted organic components and to separate Si from SiC by using the following procedure: i) first, an acetone wash was applied to the slurry to remove glycol solution, ii) second, acid dissolution with HNO_3 solution was used to remove Fe particles, iii) third, Si and SiC were separated based on their density difference using a heavy liquid of sodium polytungstate in water with a density of 2.8 g cm^{-3}, and iv) finally, Si and SiC were washed with water. XRD and wavelength dispersive X-ray fluorescence (WDXRF) showed that even after the four-step washing procedure, some metallic particles remained in the final product: such particles might be beneficial for the enhancement of the thermoelectric performance of materials.[51,52] The presence of SiC and metallic impurities was confirmed by transmission electron microscopy (TEM) characterization (**Figure 5**a–c). Cold pressed pellets of the mixed powders were heated up twice to 973 K. The products were ground and finally hot pressed under 50 MPa at 1100 K into pellets with high density of typically >97%.

Thermoelectric characterization of the samples made from sludge Si showed a higher carrier concentration (3.1 to 3.6 × 10^{20} cm^{-3}) than that in the samples made from pure Si with a similar chemical composition (≈2 × 10^{20} cm^{-3}).[50] The samples synthesized using sludge Si had higher maximum PFs than those synthesized from pure Si (Figure 5d), which could be mainly attributed to their higher σ originating from higher carrier concentration and mobility.[53–55] Fanciulli et al.[52] confirmed that the mobility is increased by the presence of a small amounts of fine metallic particles dispersed within the main material. However, κ of KERF samples was significantly higher than that of the samples synthesized using pure Si. This could be attributed to the presence of impurities such as SiC and metallic particles with high κ in the matrix phase of the studied materials. To better evaluate the contribution of SiC and metallic particles, Mesaritis et al.,[40] estimated the lattice thermal conductivity via the subtraction of electronic contribution for the total thermal conductivity using the Wiedemann–Frantz law ($\kappa_e = L\sigma T$, where L is the Lorentz factor). They observed clearly that the lattice thermal conductivity is higher for the KERF samples due to the contribution of the high thermal conductivity SiC material. This agrees with the observations of Inoue et al.[56] and Yin et al.[57] that SiC particles were responsible for the observed increase of κ of Mg_2Si-based TE materials. However, this increase in κ conflicts with the previously reported reduction in κ_l of $Mg_2Si_{0.7}Ge_{0.3}$ by the addition of SiC nanoparticles.[58] This inconsistency could be

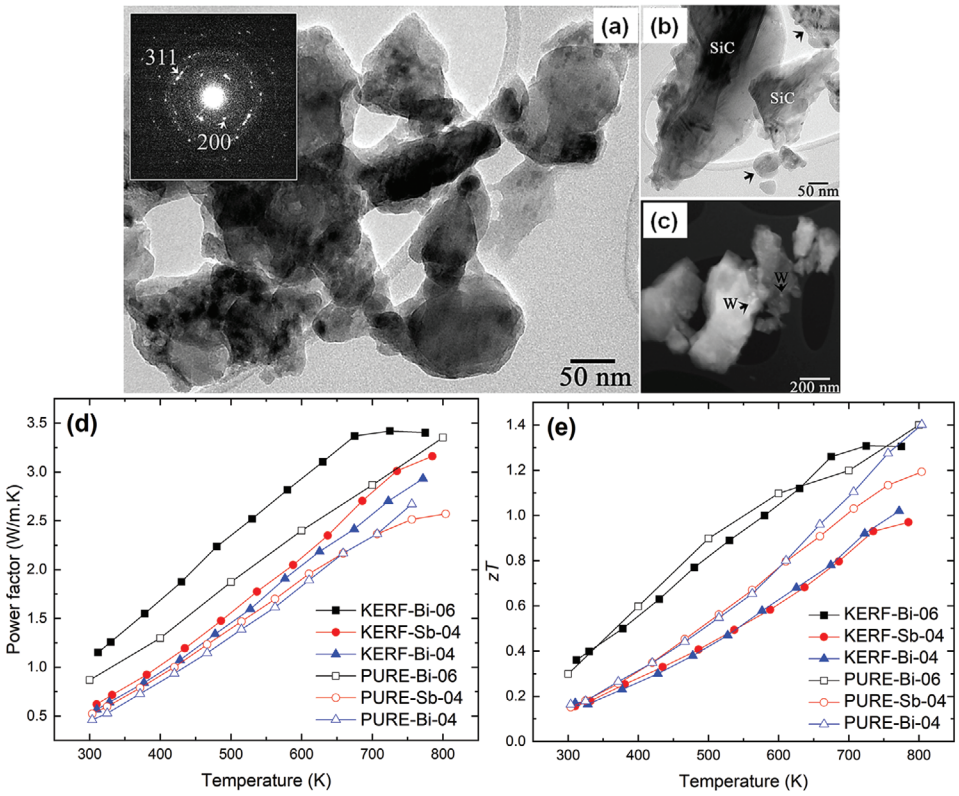

Figure 5. TEM characterization of Sb-doped Si-rich $Mg_2Si_{0.55}Sn_{0.4}Ge_{0.05}$ (KERF-Sb-Sn_{04}) particles synthesized from sludge Si. a) The matrix phase as confirmed by selected area electron diffraction (SAED) patterns in the inset, b) large SiC particles intermixed with $Mg_2Si_{1-x-y}Sn_xGe_y$ particles indicated with black arrows, and c) high-angle annular dark field (HAADF) STEM image from tungsten nanoparticles on top of $Mg_2Si_{1-x-y}Sn_xGe_y$ Sn-rich phase particles. d) PF and e) zT of Mg_2Si-based TE materials as a function of temperature. KERF and PURE are indicative of the source of Si. Bi-06, Sb-04, and Bi-04 are Bi-doped-Sn-rich $Mg_2Si_{0.4}Sn_{0.6}$, Sb-doped-Si-rich $Mg_2Si_{0.55}Sn_{0.4}Ge_{0.05}$, and Bi-doped-Si-rich $Mg_2Si_{0.55}Sn_{0.4}Ge_{0.05}$, respectively. Reproduced with permission.[40] Copyright 2019, Elsevier.

explained by the fact that the Mesaritis et al.[40] study documented micrometer-sized SiC particles. Samples synthesized from sludge Si can reach $zT \approx 1$ and 1.3 depending on their chemical composition (Figure 5e). Given that the starting material consists of waste-derived Si, the obtained values are quite high.

2.1.3. Diatomaceous Earth

It is well established that nanograined TE materials with microstructural complexity show an enhanced energy-conversion performance.[59–63] Many theoretical and experimental approaches have confirmed that both a decrease in κ and an increase in the PF can be observed in nanostructured TE materials relative to the corresponding bulk systems.[63,64] This enhancement can be attributed to interface effects, which scatter phonons more effectively than electrons, thereby increasing zT.[65] However, the use of low cost, abundant, and intrinsically nanostructured starting materials can potentially decrease the high fabrication cost of nanomaterial synthesis.[66–68]

In this context, Szczech and Jin[69] proposed using diatomaceous earth as a Si source for synthesizing nanostructured TE silicide materials. Diatomaceous earth is an abundant, inexpensive, and nontoxic nanostructured silica, composed of microshells of unicellular algae.[70] This commercially available material is used for filtering applications in the food and pharmaceutical industry.[71] The following two-step reaction of SiO_2 with pure Mg was proposed to synthesize Mg_2Si from diatomaceous earth while keeping its unique structure intact during the fabrication process

$$SiO_2(s) + 2Mg(g) \rightarrow 2MgO(s) + Si(s) \quad (3)$$

$$2Mg(g) + Si(s) \rightarrow Mg_2Si(s) \quad (4)$$

Based on the results, an optimal Mg gas displacement of 888 K for 6 h was suggested. Using a simple and practical method of Mg gas replacement, it is feasible to completely convert SiO_2 diatoms (single-celled algae) to the nanocomposite of Mg_2Si and MgO with estimated Mg_2Si grain sizes of 20–36 nm (**Figure 6**). The basic morphology and original nanocrystallinity of the starting diatom material were also preserved after the conversion.

However, as discussed above (Section 2.1.2), the presence of MgO as an impurity can deteriorate the TE performance of final material. MgO is an inherent by-product of this reaction and it cannot be removed easily from Mg_2Si by acid treatments. In order to overcome this problem, Hayati-Roodbari et al.[72] recently proposed a two-step synthesis procedure to convert meso/macroporous silica to macroporous magnesium silicide monoliths throughout gaseous magnesium–vapor reaction with macro/mesoporous silicon. In this method, highly porous Si

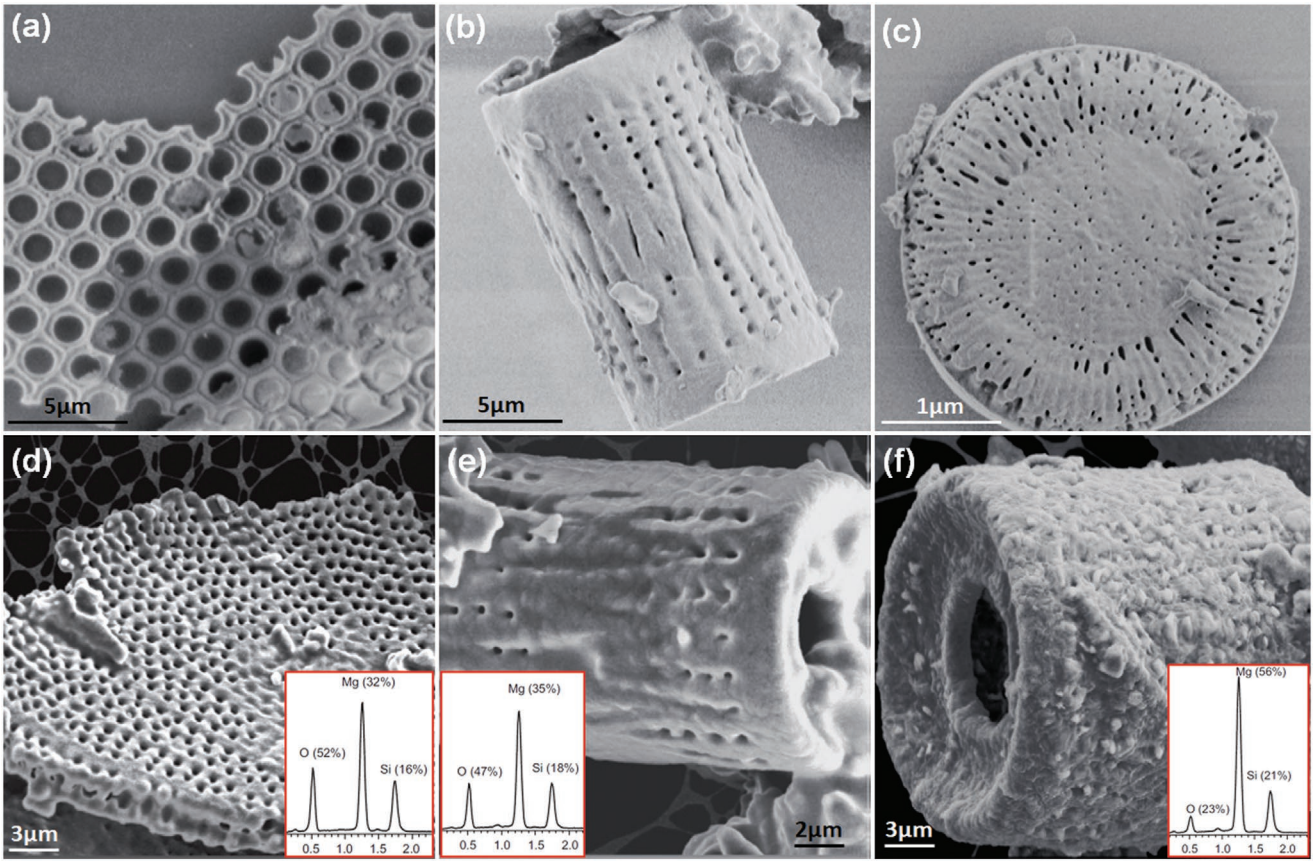

Figure 6. a–c) SEM images of various species of diatoms prior to reduction with Mg vapor; their unique and hierarchal structure includes interlocking fingers and nanoscale pores. d–f) SEM images of the converted diatom products after reduction at 888 K, with their corresponding EDS spectra. Little degradation of starting morphology can be observed in (d) and (e), while their EDS show high amount of oxygen, indicating a mixture of Mg_2Si, Si, and MgO. The image and EDS shown in (f), indicate filing of nanopores, but complete conversion to the Mg_2Si and MgO composite. Reproduced with permission.[69] Copyright 2008, Elsevier.

monoliths were first prepared by magnesiothermic reduction of a meso/macroporous silica network. In the second step, a reaction of the obtained Si monoliths with Mg vapor was induced to give a cellular network of pure Mg_2Si crystallites. Because the essence of the starting materials—their chemical composition and their porous nature—are similar in Szczech's and Hayati's studies, this recent method might be applicable to reduce the amount of MgO phases when attempting to synthesize pure Mg_2Si.

2.1.4. Opportunities and Challenges in Synthesizing Waste-Based Mg_2Si Materials

The overview presented above and the summary in Table 1 indicate that waste materials, especially waste Si, have potential as cheap and abundant sources for the synthesis of Mg_2Si. However, the role of impurities such as SiC, MgO, and metallic particles needs to be investigated further in order to develop and establish a systematic and effective methodology to use them in in synthesis of high zT materials. However, the silica-based waste materials such as rice husk and diatomaceous earth might prove to be challenging starting materials because of the formation of an MgO phase. This challenge could be overcome by using multi-step methods, such as in Hayati's work, but doing so might increase the synthesis cost which negates the cost advantage of using waste materials.

2.2. SiC-Based TE Materials from Waste

SiC, is considered as a potential thermoelectric material for use at high operating temperatures because of its high melting point, high mechanical strength, nontoxicity, and high *S*. However, its high κ leads to a low zT. To decrease κ, several methods such as porous SiC and doping with elements with good electric conductivity (such as Au, C, etc.) have been proposed.[73,74]

Although Lee and Cutler first synthesized SiC from rice husk in the 1975,[75] Takeda et al. synthesized β-SiC by carbothermal reduction of silica obtained from rice husk ash and studied its TE properties in 1993.[76] They first calcinated rice husk at temperatures from 500 to 973 K in air, which was followed by further calcination at 1273 K for 4 h. This yielded ash consisting of cristobalite silica with traces of tridymite silica. A mixture of four parts of C and one part of SiO_2 was reduced carbothermally at a temperature of 2073 K for 93 h under an Ar atmosphere, following the Acheson method.[77] The excess

Table 2. Summary of properties of SiC-based TE materials obtained from different waste sources.

Type	Chemical composition	Waste source	σ [Ω^{-1} cm^{-1}]	S [μV K^{-1}]	PF [W m^{-1} K^{-1}]	κ [W m^{-1} K^{-1}]	zT max.	Temp. [K]	Ref.
n	β-SiC	Rice husk	23.82	−225.93	0.13	–	–	1273	[76]
		High-purity Si	103.45	−119.87	0.24	–	–	1341	
		Rice husk	≈79.04	−155.95	0.19	–	–	1000	[81]
		Rice husk	–	–	≈0.4	≈8	≈0.05	1000	[84]

and unreacted graphite was then removed by further heating of the powder for 1 hour at 1073 K in air. The synthesized β-SiC powders were compacted and sintered at 2373 K for 2 h to make a porous β-SiC piece. Takeda et al. reported that SiC made with rice husk ash had a lower σ than that of pure SiC, probably because of sintering with relatively low relative density (40.3%) than that for pure SiC (61.4%). Negative values for S were obtained for both samples (SiC from rice husk ash and pure SiC), which is characteristic of n-type semiconductors. Moreover, the absolute value of S obtained for SiC from rice husk ash was higher than that of pure SiC and increasing with increasing temperature. As mentioned earlier, bulk SiC is a material with high κ: at low temperatures κ depends on the grain size of SiC.[78,79] However, Koumoto et al.[80] reported that the κ of porous SiC could be even lower than about one-tenth of the values reported for fully dense SiC ceramics, whereas σ was found to be comparable to or even higher than that of SiC single crystals.

Maeda and Komatsu[81] used a different method developed in their group for the synthesis of n-type β-SiC from rice husk ash. Rice husks were first impregnated with Fe as a reaction catalyst and sintering aid with the weight ratio of Fe_2O_3/SiO_2 = 0.043.[82,83] Both silica and carbon in rice husk were then made to react directly at high temperatures (2173 to 2473 K) using hot pressing in an N_2 atmosphere. The variation of compacting pressure and hot-pressing temperatures determined the bulk density of final porous bodies (0.5–1.7 g cm^{-3}). An increase in the nitrogen-gas pressure caused a decrease in S and an increase in σ and thereby had a direct effect on the TE performance of SiC. The authors related this to an increase in the number of charge carriers. The compacting pressure had no effect on the S, whereas it led to an increased in σ. Both S and σ increased with increasing hot-pressing temperature up to 2423 K. The researchers concluded that the best performing porous silicon carbide was obtained under the following conditions: compacting pressure of 14.7×10^6 Pa, sintering temperature of 2423 K, and nitrogen-gas pressure of 1×10^5 Pa.

In 2002, Maeda et al.[84] investigated the effect of nitrogen-gas pressure variation on the TE performance of porous SiC derived from rice husk ash. They chose the most favorable processing conditions as mentioned above, to synthesize the SiC and fabricate a sintered body from it. The nitrogen pressure varied from 0 to 4×10^5 Pa. The highest σ of 200.4 Ω^{-1} cm^{-1} at 633 K was obtained for the sample sintered at the nitrogen gas-pressure of 1×10^4 Pa: this σ value was ten times higher than the value reported by Takeda et al. (18.9 Ω^{-1} cm^{-1} at 606 K).[76] Maeda et al. attributed this increase to the insignificant formation of stacking faults in their method of synthesis of β-SiC from rice husk. The XRD and SEM characterization revealed that the nitrogen gas acted as a donor to increase the σ but, beyond 1×10^4 Pa, nitrogen assisted in the formation of Si_3N_4 and acted as a grain-growth inhibitor during the sintering. Finally considering the optimized conditions (nitrogen gas-pressure of 1×10^4 Pa), a zT = 0.055×10^{-3} was obtained. As can be observed in **Table 2**, among all SiC obtained from rice husk using different synthesis conditions, these processing conditions lead to the highest power factor.

For comparison, PF values obtained for SiC derived from rice husk are plotted in **Figure 7** as a function of studied temperature. Since different parameters were studied in the work of Maeda,[81,84] best PFs obtained for each parameter are included in Figure 7.

Table 2 summarizes the approximate values of certain properties of different SiC-based TE materials obtained from waste. As an outlook, synthesis of nano-SiC from rice husk as a TE material can be suggested. Nanostructured TE materials have shown promising commercial use due to their remarkable thermoelectric performance and synthesis of nano SiC from rice husk as a TE material might be a new line of thought, since it can reduce the high production price of nano TE materials.[85,86] Beside rice husk, other agricultural waste materials with high silica content can be used also for synthesis porous SiC based TE materials.

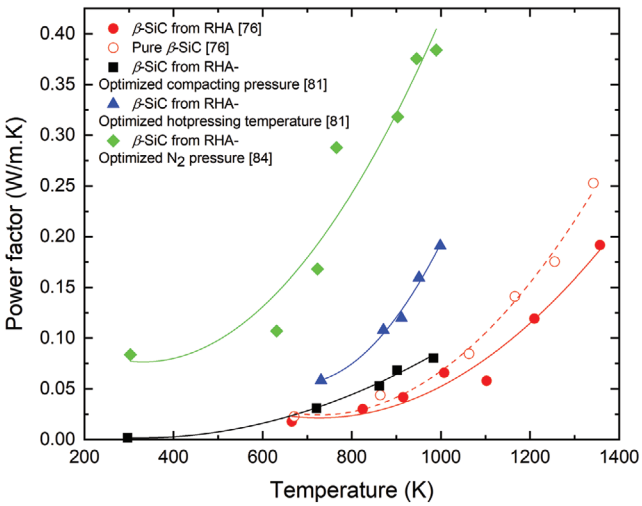

Figure 7. Comparison between PF (as a function of temperature) of β-SiC derived from rice husk and pure β-SiC.[76] For comparison, data from Maeda and Komatsu[81,84] are also included, showing the effect of gas pressure, compacting pressure, and hot-pressing temperature on PF of a sintered SiC body.

2.3. Bi_2Te_3-Based TE Materials from Waste

Since the first appearance of bismuth telluride (Bi_2Te_3) in 1956,[87] materials based on this compound are the best known TE materials for waste-heat recycling at low and ambient temperatures. The carrier concentration in Bi_2Te_3 can be tuned by alloying with Sb_2Te_3, yielding a p-type composition close to $(Sb_{0.8}Bi_{0.2})_2Te_3$, whereas the composition of the n-type compound is approximately $Bi_2(Te_{0.8}Se_{0.2})_3$. The κ of bismuth telluride can also be minimized by microstructure engineering and nanostructuring.[88–91] Bi_2Te_3 materials are already used in thermoelectric refrigeration, TEGs, and thermal sensors.[92,93]

Elements like Se and Te are expensive because of their limited reserves and the increased use in metallurgy (improving machinability of steel and copper with Te), chemical industry (Te as a vulcanizing agent and accelerator in the processing of rubber and as a component of catalysts for synthetic fiber production), pigments, and photovoltaic industries. Moreover, Bi_2Te_3-based TE materials have been used for almost seven decades, also contributing to the demand. The effects of this demand can be seen in the fact that the unit prices of Te and Se skyrocketed from \$38.00 to \$79.00 kg^{-1} and 10.78 to 20.00 kg^{-1}, respectively, from 2017 to 2018.[94]

Despite the scarcity and cost, Te recycling is still very limited because of its use in dissipative applications, i.e., one that cannot be effectively or economically collected and processed. For instance, only a small amount of Te is recovered from discarded selenium-tellurium photoreceptors used in older plain-paper copiers in Europe. Also, only limited Te can be recovered from CdTe solar cells, since most CdTe solar cells are in operation for only a few years and have not yet reached the end of their useful life. Te and Se can be recovered by using hydrometallurgy, but in small quantities and only after a long and polluting process. Therefore, the establishment and development of methods to recover these scarce elements from wastes or use wastes from other sources in the synthesis Bi_2Te_3-based TE materials are of great importance, both economically and environmentally. In the following sections, we review the different waste sources that can be used to synthesize Bi_2Te_3-based TE materials.

2.3.1. Discarded Bi_2Te_3 Pieces and Powders

Considerable waste is generated during the production and processing of Bi_2Te_3 ingots. During the growth of ingots, both sides of an ingot are cut and discarded because of inhomogeneity in its chemical composition. An additional 30% of material is also lost during the subsequent processing, such as cutting and assembling, because of the intrinsic brittleness of Bi_2Te_3.[95]

In 2008, a new approach to the recycling of Bi_2Te_3 waste powders was proposed by Tritt's group.[95–97] They postulated that it would be possible to reduce κ without scarifying the σ of TE materials by using grain boundary engineering. They first applied an alkali-metal salt nanocoating on polycrystalline p-type Bi_2Te_3 powders via a hydrothermal technique. A thin layer of alkaline metal (Na, K, and Rb) was formed around the particles (see **Figure 8**) and later became part of the grain–boundary phase during compaction by hot-pressing. Although no experiments were done on Bi_2Te_3 waste powders, the results on ground powders obtained from a Bi_2Te_3 ingot ($Bi_{0.4}Sb_{1.6}Te_3$) showed that the thin film helped the development of a thermoelectrically favored grain boundary.[96]

Zu[95] reported that an optimal molar ratio of Na:Rb = 1:2 made a polycrystalline sample capable of obtaining the same zT as a commercial ingot. Based on the results obtained for the ground ingots, hydrothermal treatment can be inferred to be a suitable way of recycling of Bi_2Te_3 waste generated during the mechanical processing of the brittle ingot.

In a series of experiments, Fan and co-workers[98–100] used different types of wastes discarded during the industrial synthesis of Bi_2Te_3 ingots as raw materials to prepare p-type Bi_2Te_3-based TE materials. The wastes were powders and fragments resulting from cutting Bi_2Te_3 wafers and particles resulting from cutting process of zone melting.[98–100] The waste powders obtained from the cutting of wafers contained high amounts of carbon and oxygen, which came from the linear cutting liquid, and oxides of Bi, Te, and Sb (**Table 3**). All the waste materials were washed with deionized water and absolute ethyl alcohol to remove the contamination by the linear cutting liquid. Depending on the level of oxygen, either hydrogen reduction at 1103 K for 1.5 h or vacuum reduction at 100 Pa at 923 K for 30 min were performed on the powder samples and fragments. For the waste obtained from the cutting of zone melting, two methods of carbon monoxide reduction (943 K, 60 min, and flow rate of 800 ml/min) and vacuum reduction (at 943 K for 30 min at 100 Pa), were applied. The EDS analyses after reduction showed significant decrease in the oxygen content of waste materials. In all cases, element adjustment was done to tune the carrier concentration of $(Bi, Sb)_2Te_3$ alloys. Various alloys with different chemical composition were prepared from each waste source for TE

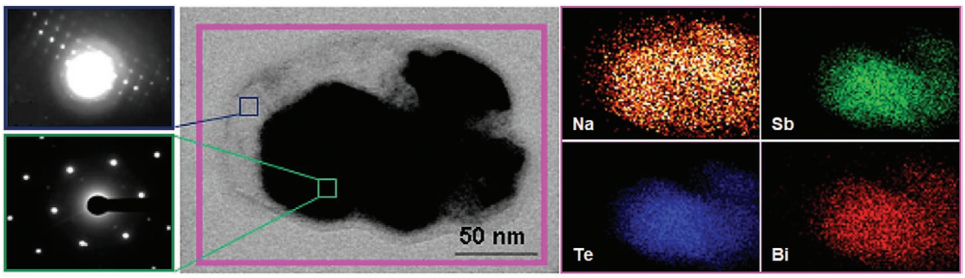

Figure 8. TEM image of coated $Bi_{0.4}Sb_{1.6}Te_3$ particle after Na hydrothermal treatment. Blue and green selected areas show the SAED patterns of the Na-contained surface layer and the $Bi_{0.4}Sb_{1.6}Te_3$ particle, respectively, while EDS mapping (pink selected area) confirms presence of Na. Reproduced with permission.[96] Copyright 2008, American Institute of Physics (AIP).

Table 3. Nominal chemical composition and nomenclature of the different wastes and obtained compounds studied by Fan and co-workers[98–100].

Waste	Chemical composition of Bi_2Te_3 waste [wt%]		Chemical composition of obtained TE materials	Nomenclature
A	C	20.23	Initial	AI
(waste powders from cutting	O	39.83	reduction/smelting	ANA
Bi_2Te_3 wafers)	Sb	18.50	$Bi_{0.36}Sb_{1.64}Te_3$	A1
	Te	15.89	$Bi_{0.4}Sb_{1.6}Te_3$	A2
	Bi	5.54	$Bi_{0.44}Sb_{1.56}Te_3$	A3
B	C	–		
(waste fragments from cutting	O	17.75		
Bi_2Te_3 wafers)	Sb	23.97	No adjustment	BNA
	Te	47.27	$Bi_{0.4}Sb_{1.6}Te_3$	B2
	Bi	11.01		
C	C	–		
(waste particles from the cutting	O	18.87	No adjustment	CNA
process of the zone melting)	Sb	23.46	$Bi_{0.36}Sb_{1.64}Te_3$	C1
	Te	47.09	$Bi_{0.4}Sb_{1.6}Te_3$	C2
	Bi	10.58	$Bi_{0.44}Sb_{1.56}Te_3$	C3

characterization (Table 3). After milling the ingots into powders with size of 38 µm, the ground powders were subjected to resistance pressing sintering (RPS) at different temperatures in argon atmosphere.

The AI sample (partially reduced and sintered waste powder) had the lowest PF and zT among all the samples (**Figure 9**). This could have resulted from the presence of oxide phases such as sub-micrometer-sized Bi_4TeO_8 granules and cubic Sb_2O_3, which acted as scattering centers for carriers increase the carrier–grain boundaries scattering and reduce the mobility (μ) and thus σ (because $\sigma = ne\mu$). Further, through the complete reduction and composition correction in all samples, PF and zT increased considerably because both n and μ increased. Finally, an increase in the Sb content caused a significant increase in the σ of the reduced samples, as reported in other literature.[101,102] Based on the obtained S, the doped Sb caused a change in the conducting behavior from n-type to p-type as compared to the initial waste powders derived from wafer cutting and waste particles from the cutting process of the zone melting (wastes A and C).

The maximum zT value of 1.16 was obtained for the $Bi_{0.44}Sb_{1.56}Te_3$ sample derived waste powders from wafer cutting at 363 K (Figure 9b). Furthermore, the average zT value of all compounds derived from waste sources were more than 0.8 which make these new recycling technologies quite promising and applicable to a vast variety of waste products such as tops and tails of single crystal bars, broken irregular square particles, and cutting debris.

2.3.2. Waste Carbon Fibers

Since the emergence of carbon fiber reinforced composite in the late 20th century, the amount of discarded and wasted composite became a matter of great concern. Many attempts were made to prevent filling landfills up by waste composites and also to conserve resources that were used to form these composites.[103,104] Yet, despite much progress with TE materials, the lack of flexibility proved to be the Achilles Heel: this restricted their application in settings in which conformability and pliability of the generator with the heat source matters. To overcome this limitation, either fully organic TEs or inorganic/organic hybrids could be used.[105–107] Carbon fibers possess high σ and low but tunable S: the latter might be improved

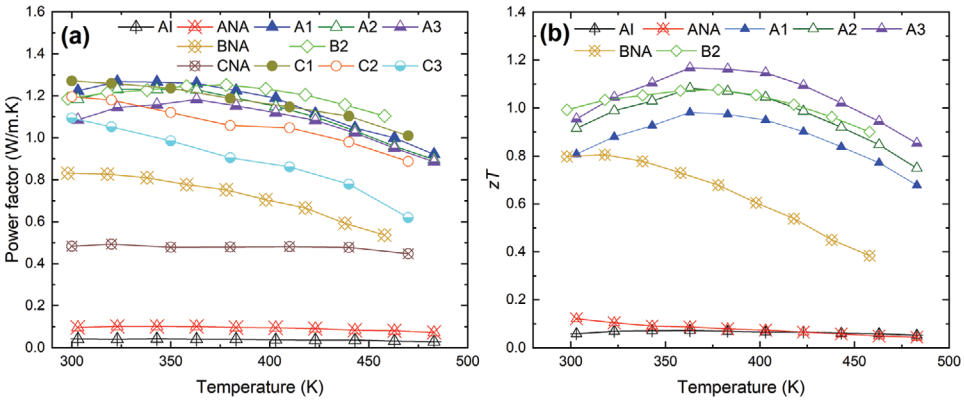

Figure 9. a) PF and b) zT values of samples obtained from different waste sources with different nominal stoichiometry. κ values of Bi_2Te_3 alloys starting from waste particles derived from the cutting process of the zone melting (waste C) are not reported; therefore, zT values of the final compounds are not reported in (b).[98–100] The legends are for both (a) and (b).

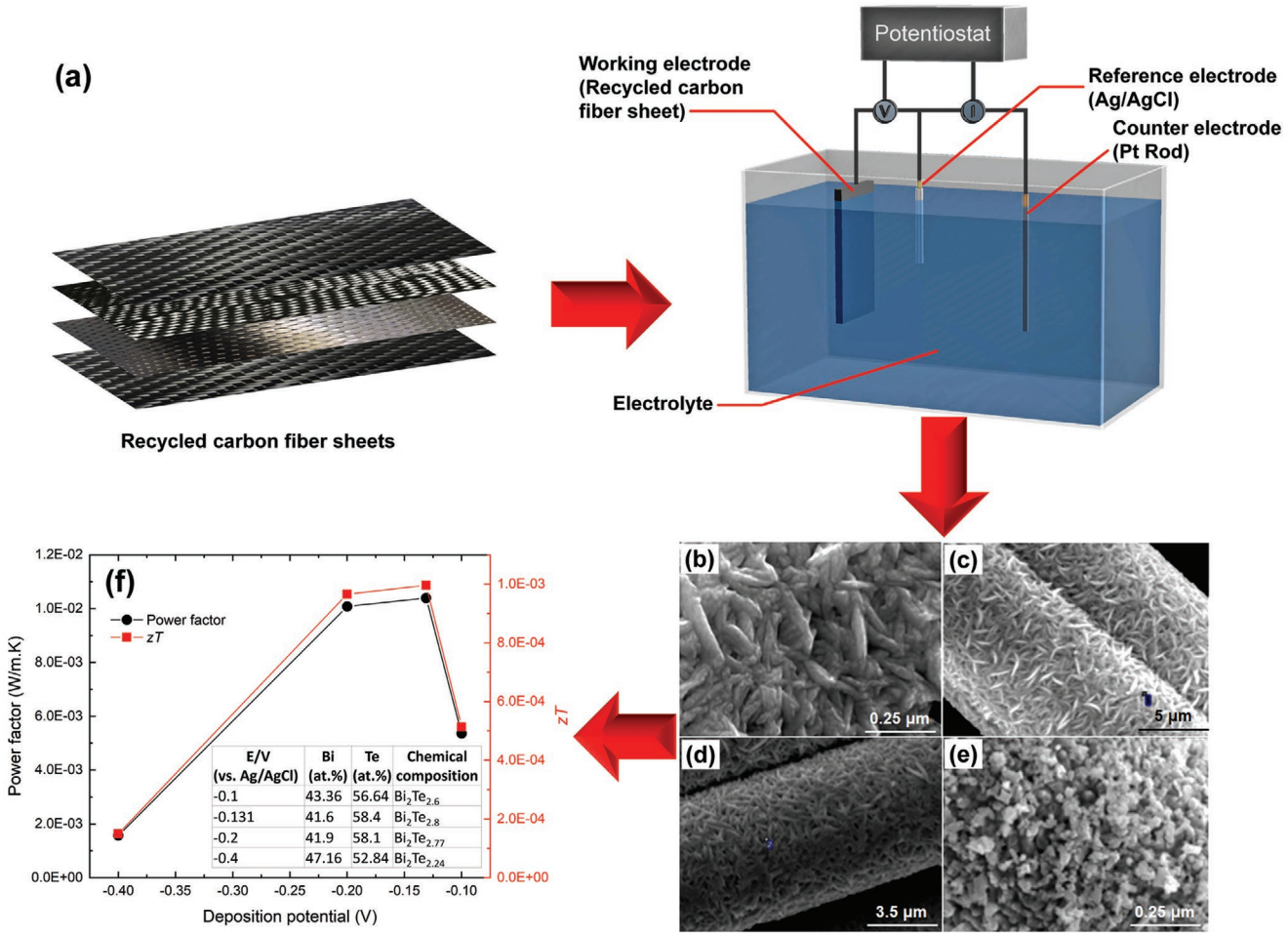

Figure 10. a) Schematic of the standard three-cell electrode setup used for the deposition of Bi_2Te_3 on carbon fiber in Pang's study. SEM images of the various Bi_2Te_3 deposited at deposition potential of b) −0.1, c) −0.131, d) −0.2, and e) −0.4 V, f) PF and zT of Bi_xTe_y-coated recycled carbon fiber sheet as a function of deposition potential. zT values calculated assuming carbon fiber's κ value. Reproduced with permission.[108] Copyright 2012, Elsevier.

by using the doping/coating process, which is similar to some extent to the semi-conductor doping process.

In 2012, Pang et al.,[108] presented an innovative idea to reutilize recycled carbon fiber (RCF) in combination with TE coatings as a flexible TE material (**Figure 10**). The carbon fiber used in their study was recycled from a toughened epoxy composite scrap via a pyrolysis process and was then shaped into a sheet by using a standard wet papermaking method. Using the technique of electrodeposition, Bi_2Te_3 films were deposited on RCFs from aqueous nitric acid containing bismuth (III) nitrate pentahydrate ($BiN_3O_{9.5}H_2O$) and telluriumoxide (TeO_2), as follows

$$3HTeO_2^+ + 2Bi^{3+} + 9H^+ + 18e^- \rightarrow Bi_2Te_3 + 6H_2O \quad E^0 = 0.483 \text{ V versus NHE} \tag{5}$$

TE characterization of the Bi_2Te_3-coated RCF showed that the maximum zT of 9.96×10^{-4} was obtained for the compound deposited with an electrodeposition potential of −0.131 V. Also, the chemical composition of the different coatings showed that the sample with the composition closest to the perfect composition of Bi_2Te_3 possessed the highest zT and PF among all deposited films (see Figure 10).

Recently, Jagadish et al.[109–111] pursued the idea of applying TE materials on RCF by different methods and investigated the effect of different deposition parameters on TE performance of the final composites. Similar to Pang et al.,[108] the TE compound was deposited on carbon fibers using electrodeposition. The results showed that the maximum S of −13.42 µV K^{-1} was obtained by using an optimized deposition condition (deposition potential: −0.10 V; deposition time: 30 min; deposition temperature: 298 K; and (Bi/(Bi+Te)): 0.240). The absolute value of the obtained S was significantly less than that of similar TE composite (−37 to −53 µV K^{-1}).[108] In the latest study, they applied a coating of Bi_2Te_3 and Bi_2S_3 on recycled carbon fiber to make a TE composite.[109] Using the brushing technique, a suspension of TE particles (15–60 wt%) with ethylene glycol and Acrodur DS 3530 binder was applied on recycled carbon fibers. PF increased as the content of the TE powder in the composite increased (up to 45 and 60 wt%, for RCF–Bi_2Te_3 and RCF–Bi_2S_3 composites, respectively), following which the PF remained almost constant (**Figure 11**). The highest PF values of 60.72 ± 3.03 and 29.45 ± 1.47 µW m^{-1} K^{-1} were obtained for RCF–Bi_2Te_3 and RCF–Bi_2S_3 composites, respectively.

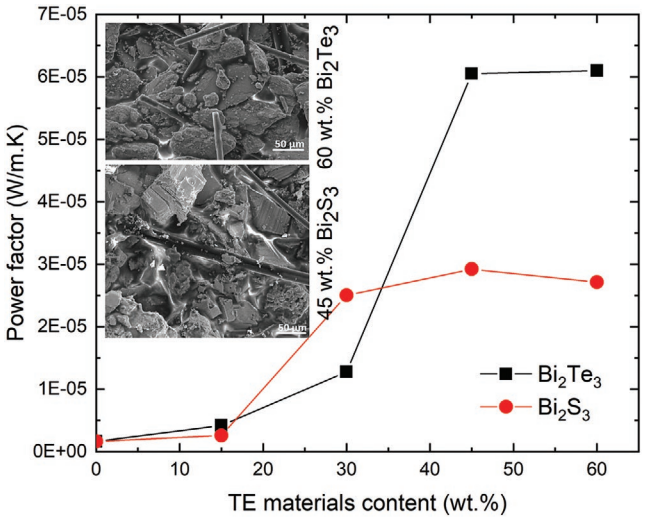

Figure 11. PF of TE composite as a function of weight percentage of TE materials. The insets are microstructure of composite with 60 wt% Bi_2Te_3 and 45 wt% of Bi_2S_3, which yield the highest PFs. Reproduced with permission.[109] Copyright 2018, Elsevier.

2.3.3. Copper Extraction Byproducts

Besides metallurgical methods to synthesize Bi_2Te_3 alloys, chemical routes such as coprecipitation, solvothermal reaction, metal-salt reduction, etc., are used to synthesize Bi_2Te_3 with higher molar ratios accuracy of Bi–Te, such as 2:3, rather than that observed in the synthesized alloys using the metallurgical melt process.[112–114] However, it should be noted that metal precursors used to synthesize TE materials are expensive and make the chemical processes as expensive as metallurgical melt process.

The Cu smelting process is used to separate elemental copper from copper concentrates through multiple sulfide-oxidizing stages.[115] Apart from silicates and copper, the Cu smelting slag typically contains Fe, Zn, Se, Te, Sn, Ni, Cd, Co, Sb, Ag, Au, Pt, and Pb. The gaseous waste stream from the smelter/convertor typically contains Ge, Bi, Hg, Pb, Cd, Sn, Zn, Se, and Te.[116] Moon Lee et al.,[117] used byproducts generated during the Cu smelting process for the preparation of a Te precursor (TeO_2). TeO_2 was obtained from the solution through a series of extraction processes, explained in detail in their study.[117] Bi_2Te_3 powders were synthesized using a wet chemical process, which involved the reaction between aqueous solutions of 0.1 M bismuth chloride and 0.1 M tellurium oxide, followed by washing and heat treatment of the precipitated powders at 673 K for 6 h in H_2 atmosphere. The XRD results showed that the Bi_2Te_3 samples synthesized using the recycled precursor were free from unwanted phases such as the ones observed in the samples fabricated using a commercial precursor of TeO_2. Therefore, it can be concluded that using the method proposed by Lee et al.,[117] it is possible to obtain a large amount of Te precursor from the waste solution generated during the copper smelting process.

2.3.4. Opportunities and Challenges in Synthesizing Waste-Based Bi_2Te_3 Materials

As discussed in this section, most of the attempts to use waste materials in synthesizing Bi_2Te_3 have focused on using the waste and intermediate product generated during the synthesis of Bi_2Te_3 ingots. Nowadays, clean production, recycling, and respect to the environment are the key factors when developing new technology and ensuring its sustainable growth matters. Regarding the idea of using RCF as a support for TE coating, as a window of opportunity, the Te precursor can be obtained using the method proposed by Lee et al.[117] In this way, both composite constituents can be derived from waste materials. **Table 4** summarizes approximate values of certain properties of different Bi_2Te_3-based TE materials obtained from wastes as well as similar compositions obtained from pure starting materials.

2.4. Other TE Materials from Waste Materials

In addition to SiC, Mg_2Si, and Bi_2Te_3, some studies also used cast-iron scrap to synthesize iron disilicide or Si waste as TE materials. Huge amount of cast-iron scrap is generated during the mechanical processing of cast iron. Since cast iron consists mainly of iron with carbon and silicon, its scrap chips are expected to be a good starting material for synthesis of iron-based TE materials, although this application cannot be considered as a method for utilizing large volumes of waste. Semiconducting iron disilicide (β-$FeSi_2$) is renowned as an attractive TE material because of its availability in both n-type and p-type semiconductors, its high S, low cost and toxicity, and its excellent resistance against oxidation.[118,119] Also, among all silicides, β-$FeSi_2$ is one of the few semiconductors which possesses a tunable band gap, which is promising for TE, optoelectronic, and photovoltaic applications.[120,121]

Recently, Laila et al. proposed to use cast-iron scrap chips as a starting material for the synthesis of β-$FeSi_2$ TE material.[122,123] GDMS analyses revealed the presence of silicon (2.2 wt%), carbon (2 wt%), and iron as the main constituents of the scrap chips, in addition to some minor elements (Mn, Mg, S, P, etc.). Cast-iron chips were used directly with Si and doping elements (Co, Mn, and Al) in the synthesis of TE materials using milling and pulsed electric current sintering techniques. Besides the formation of β-$FeSi_2$, the presence of trace amounts of ε-FeSi phase was also confirmed by XRD. According to the literature, p-type $FeSi_2$ can be obtained by doping with transition elements, such as Mn and Cr, that lie on the left side of Fe in the periodic table, or doping Si substitution by Al. Doping with elements such as Co and Ni, which lie to the right of Fe, yields n-type material.[124] As shown in **Figure 12**, doping with substitution concentration of 0.08 Mn, 0.09 Al, and 0.06 Co led to the maximum zT values of 0.17, 0.1, and 0.22 at 1073, 773, and 973 K, respectively. The comparison with the values reported in the literature for the similar nominal compositions[125–128] shows that the cast-iron scrap chips are effective as a starting material for synthesis of β-$FeSi_2$ and are capable of producing a material comparable to conventional β-$FeSi_2$ fabricated from pure Fe.

Table 4. Summary of properties of Bi_2Te_3-based TE materials obtained from different waste sources and doped by different dopants.

Type	Chemical composition	Waste source	σ [Ω^{-1} cm^{-1}]	S [μV K^{-1}]	PF [W m^{-1} K^{-1}]	κ [W m^{-1} K^{-1}]	zT max.	Temp. [K]	Ref.
n	$Bi_2Te_{2.6}$	Bi_2Te_3-coated RCF	120	−37.76	0.5×10^{-2}	–	5.1×10^{-4}[a)]	313	[108]
	$Bi_2Te_{2.8}$	Bi_2Te_3-coated RCF	138	−48.96	1.03×10^{-2}	–	9.9×10^{-4}[a)]	313	
	$Bi_2Te_{2.77}$	Bi_2Te_3-coated RCF	112	−53.56	1.00×10^{-2}	–	9.7×10^{-4}[a)]	313	
	$Bi_2Te_{2.24}$	Bi_2Te_3-coated RCF	30	−40.66	1.6×10^{-3}	–	1.5×10^{-4}[a)]	313	
	As received	Powders from cutting Bi_2Te_3 wafers	78.04	−127.35	4.3×10^{-2}	0.62	0.069	363	[98]
	Reduced	Powders from cutting Bi_2Te_3 wafers	277.45	−101.61	0.1	0.86	0.11	363	
	Carbon monoxide reduced	Cutting process of the Bi_2Te_3 zone melting cutting waste powders	802.02	−142.1	0.48	–	–	300	[100]
P	Na-treated $Bi_{0.4}Sb_{1.6}Te_3$	Grounded ingot	514.1	220.9	0.79	1.1	0.72	323	[96]
	K-treated $Bi_{0.4}Sb_{1.6}Te_3$	Grounded ingot	554	218.5	0.85	1.22	0.70	323	
	Rb-treated $Bi_{0.4}Sb_{1.6}Te_3$	Grounded ingot	554	227.9	0.93	1.17	0.79	323	
	$Bi_{0.4}Sb_{1.6}Te_3$ (Bulk)	Pure	473.3	218.9	0.74	1.26	0.59	323	
	Vacuum reduced	Bi_2Te_3 cutting waste fragments	325.72	247.22	0.75	1.12	0.67	379	[99]
	$Bi_{0.4}Sb_{1.6}Te_3$	Bi_2Te_3 cutting waste fragments	650.98	229.75	1.25	1.17	1.07	379	
	$Bi_{0.36}Sb_{1.64}Te_3$	Cutting process of the Bi_2Te_3 zone melting cutting waste powders	1206.38	184.53	1.26	–	–	300	[100]
	$Bi_{0.4}Sb_{1.6}Te_3$	Cutting process of the Bi_2Te_3 zone melting cutting waste powders	963.76	202.27	1.20	–	–	300	
	$Bi_{0.44}Sb_{1.56}Te_3$	Cutting process of the Bi_2Te_3 zone melting cutting waste powders	703.18	226.34	1.10	–	–	300	

[a)]zT values calculated assuming carbon fiber's κ value.

As mentioned in Section 2.1.2, Si obtained from recycled sawing waste was used as a starting material to synthesize Mg_2Si compounds.[40,45,47] The similar TE performance of samples synthesized from waste Si with that of compounds synthesized from commercial-grade high-purity silicon confirms the great potential of using Si kerf for TE applications. However, He et al.[39] suggested direct utilization of recycled Si as TE material by applying industrially developed methods such as ball milling and the spark plasma sintering (SPS) technique. In order to tune the carrier concentration, phosphorous (P) was used as a dopant. They observed that carrier concentration increased significantly from 1.7×10^{18} to 2.1×10^{20} cm^{-3} with 0.1 and 2 at% P substitution, respectively. The presence of SiC, Fe, and O, as inescapable impurities in Si kerf, may affect TE performance, possibly by i) reduction of P solubility in waste Si because of induced compressive strain on Si lattice by SiC, ii) scattering the charge carriers by SiC particles, iii) the presence of P-depleted zones, because the solubility of P in SiC is negligible in comparison to that of Si, and iv) formation of complex compounds in the Si matrix. The two latter possibilities are clearly illustrated in the **Figure 13**a–f. Local electron energy loss spectroscopy (EELS) shows phosphorus incorporation into the silicon matrix (see Figure 13b,c) and also P depletion in the regions with high C concentration (SiC grains; Figure 13d). Also, the presence of Fe and O in Si matrix can be seen in Figure 13e,f.

The maximum PF value of ≈3 W m^{-1} K^{-1} at 1073 K was obtained for the recycled Si with 2 at% P substitution, which was

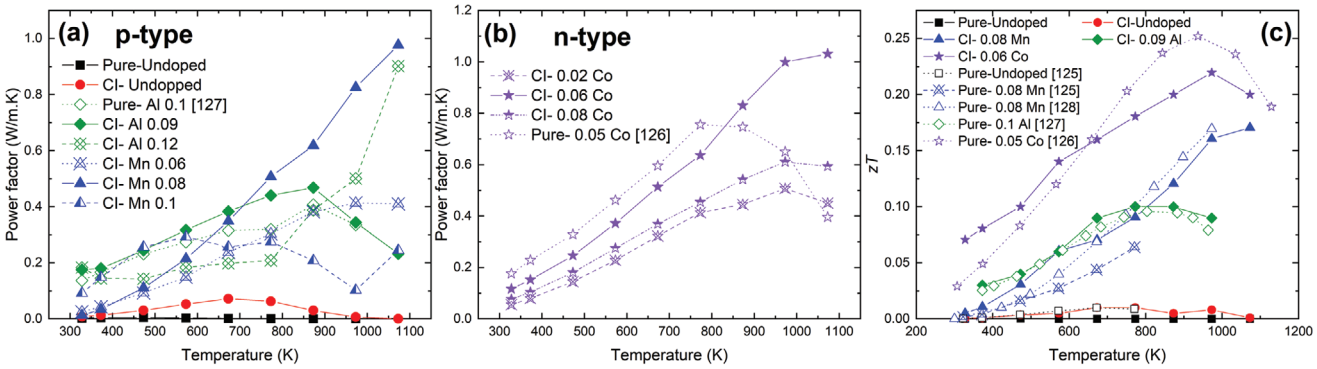

Figure 12. zT versus temperature for n-type and p-type $FeSi_2$ doped with (Mn, Al, and Co) dopants.[122,123] $Fe_{0.92}Co_{0.08}Si_2$ and $FeSi_2$,[125] $Fe_{0.92}Mn_{0.08}Si_2$,[128] $FeAl_{0.1}Si_2$,[127] and $Fe_{0.5}Co_{0.5}Si_2$.[126]

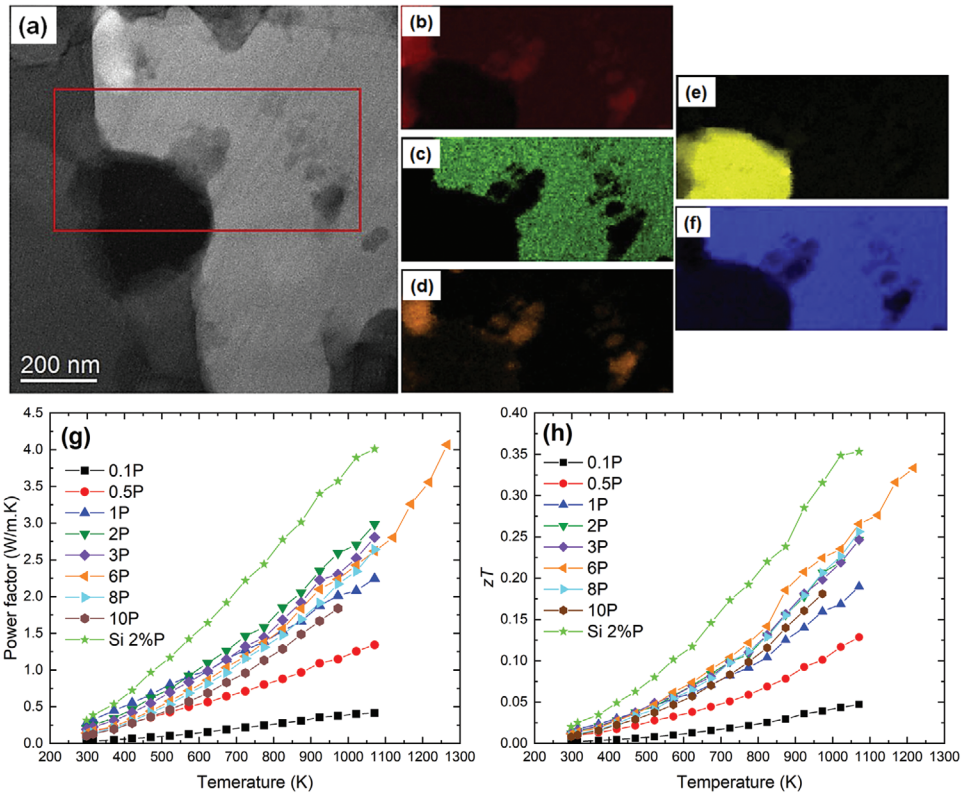

Figure 13. a) High-resolution scanning transmission electron microscopy (HR-STEM) and EELS measurements of the Si slurry sample with 10 at% P. a) Annular dark field image with marked area for local EELS measurements. Elemental maps of b) Si–L, c) P–L, d) C–K, e) O–K, and f) Fe–L, respectively, g) PF and h) zT values of P-doped recycled Si sawing waste. The TE properties of 2 at% P-substituted Si are also plotted. Reproduced with permission.[39] Copyright 2019, Elsevier.

less than that of reference Si doped with 2 at% P (3.97 W m^{-1} K^{-1}) (Figure 13g). However, higher PF of ≈4.07 W m^{-1} K^{-1} was obtained for the waste Si doped with 6 at% P at 1273 K, which is comparable to doped SiGe alloys.[129] Among all waste Si, the peak zT value of ≈0.33 was obtained for recycled Si with 6 at% P substitution at 1217 K (Figure 13h).

3. Recycling of Scarce Elements from TE Materials

As discussed earlier, the synthesis and development of TE materials from elements derived from natural raw materials entails high costs, high energy consumption, and adverse environmental consequences. One way to address this is by using various type of waste materials, as reviewed in Section 2. Another way is to use elements recycled from end-of-life (EoL) TE modules. Recycling concepts for EoL TE modules in Union Minière have been discussed by G. Knockaert, in 1993. The focus was on recycling the scrap or EoL TE modules to Bi_2Te_3 or PbTe alloys to be used readily in the production of new TE modules.[130] At present, because of environmental issues and the scarcity of elements such as Te, the new recycling methods are applied to other modules as well, since they reached to the substantial production volume. Although there is contradictory information about availability of raw elements for some TE materials such as half-heusler compounds and $CoSb_3$, the scarcity of raw materials of Bi_2Te_3, PbTe, and SiGe makes them the most expensive TE materials.[131] Today, besides high zT values, the price of raw materials for each established compound is considered as a further criterion for optimum materials. It should also be noted that some TE materials, such as PbTe-based materials, will not achieve social acceptance due to their poor solubility and environmental consequences despite significant improvements in their performance. Therefore, the main goals in recovering elements from TE materials are i) lowering the final cost of TE synthesis by use of scarce recycled material and ii) extraction of those elements from EoL products, which prevents the considerable loss of scarce materials. However, despite a rapid increase in the use of TE modules in power generation and refrigeration, only a few studies have explored methods of recycling scarce elements such as Te from TE modules.[132] Te is well distributed in the Earth's crust, but its concentration is not high enough to allow it to be mined directly. Therefore, Te is recovered as a byproduct of nonferrous metal mining, largely from the copper refining process. Most studies on element recycling have focused on recycling precious metals (e.g., Au, Ag, Pd, and Pt), scarce elements (e.g., Pt, Ir, Os, Pd, Rh, Ru, Au, Re, and Te) and rare-earth from waste electrical and electronic equipment (WEEE).[133–136] For this purpose, several approaches such as hydrazine reduction and bacterial recovery methods were proposed, which will be reviewed in this section. Following this overview, we discuss the challenges and opportunities associated with elemental recovery from EoL TE modules.

3.1. Te Recovery through Chemical Reactions

Chemical reactions, not only are used to synthesize TE materials, but they can also be applied to recycle scarce elements and even TE materials from spent TE modules.[137–139] Using a low-cost hydrazine reduction process, Kim[140] recycled nanosized Bi_2Te_3 and Te powders from waste TE modules. In this study, the TE chips separated from the TE modules were washed with acetone and an acidic solution and then dissolved in a nitric acid solution. Then, the precipitated powders and ion-containing solution were separated. In order to synthesize Bi_2Te_3 nanopowders, the ion-containing solution was reduced by hydrazine hydrate solution, while for Te nanopowders the hydrazine solutions were dropped directly onto the surface of the precipitated white powders. The formation of Bi_2Te_3 and Te powders can be explained by the following chemical reactions

i) Dissolving reactions

$$2Te + 9HNO_3 \rightarrow HTeO_2^+ + TeO_2 \downarrow + NO_3^- + 8NO_2 \uparrow + 4H_2O \quad (6)$$

$$Bi + 4HNO_3 \rightarrow Bi^+ + 3NO_3^- + NO \uparrow + 2H_2O \quad (7)$$

ii) Reduction reactions

$$2HTeO_2^+ + N_2H_2 \rightarrow 2Te + N_2 + 2H_2O + 2OH^- \quad (8)$$

$$6Te + 3N_2H_4 + 4Bi^{3+} + 12OH^- \rightarrow 2Bi_2Te_3 + 3N_2 + 12H_2O \quad (9)$$

which can be summarized as

$$3HTeO_2^+ + 3N_2H_4 + 2Bi^{3+} + 3OH^- \rightarrow Bi_2Te_3 + 3N_2 + 9H_2O \quad (10)$$

Besides the formation of Te and Bi_2Te_3 nanopowders, the formation of Sb_2O_3 was also confirmed by XRD, which might be due to a higher standard reduction potential (E^0) of TeO_2 to Te and Sb_2O_5 to Sb_2O_3 than that of Sb_2O_3 to Sb (E^0 = 0.53, 0.69, and 0.15 V, respectively). HR-TEM and fast Fourier transformation (FFT) analyses of the synthesized powders confirmed the formation of pure phases Bi_2Te_3 and Te with the particle-size range of 20–40 and 10–100 nm, respectively (**Figure 14**).

So et al.[141] attempted to recover Te from n-type Bi_2Te_3 by using a wet reduction process. They suggested immersing separated Bi_2Te_3 compounds in HCl solution to remove solder and organic impurities and a pretreatment of TE waste modules, since both n-type and p-type TE materials coexist in TE modules. For this purpose, a certain amount of both n-types and p-types were immersed in a HNO_3/H_2O solution in the ratio of 2/1 for 24 h. In this way, solid p-type chips and impurities existing in the recovered solution could be filtered easily. Then, NaOH was added to the filtered solution to adjust the pH to 13. At pH 13, $N_2H_4{\cdot}H_2O$ was added and reduction reactions were allowed to occur for 12 h at 70 °C as follows

$$6Bi + 6HNO_3 \rightarrow Bi_2O_3 + 6NO_2 + 3H_2O \quad (11)$$

$$Bi_2O_3 + N_2H_4 \rightarrow 2Bi + 2NO + H_2O + H_2 \uparrow \quad (12)$$

Once the reactions were complete, an aqueous solution containing Te ions was obtained after centrifuging and filtering, and the particles were recuperated in the form of dried powder. HNO_3 was again used to adjust the pH of the Te-containing solution to 7, and cetyltrimethylammonium bromide (CTAB) was added. Next, $N_2H_4{\cdot}H_2O$ was added for re-reduction at 70 °C. XRD and EDS analyses confirmed that Bi is the main constituent of the reduced particles at pH 13 (95.31 at% Bi), while Te with 99% purity was obtained after reduction at pH 7 (99.69 at% Te).

Recently, So et al.[142] investigated the synthesis of Te nanorods from EoL-TE modules via a hydrothermal method. In their study, two steps of chemical reactions of dissolving in HNO_3 solution and reduction with hydrazine monohydrate were applied to extract Bi particles. The Bi-separated solution as well as predissolved polyvinylpyrrolidone (PVP) and hydrazine monohydrate then were moved to an autoclave for heating to 433 K for 6 h. A small trace of Se was detected by inductively coupled plasma-optical emission spectrometry (ICP-OES), and Sb and Bi were not detected either by XRD nor ICP-OES (**Figure 15**).

3.2. Bacterial Recovery

Bacteria are already used in the bioleaching of iron and copper from their ores or in water remediation.[143–147] Bonificio and Clarke[143] reported that bacteria could also help extract Te from the EoL tellurium-based devices, such as photovoltaic (PV) modules and TE generators. In their study, they showed that the hydrothermal vent microbe *Pseudoalteromonas* sp. strain EPR3 can convert tellurium from a wide variety of compounds, industrial sources, and devices into metallic tellurium and a

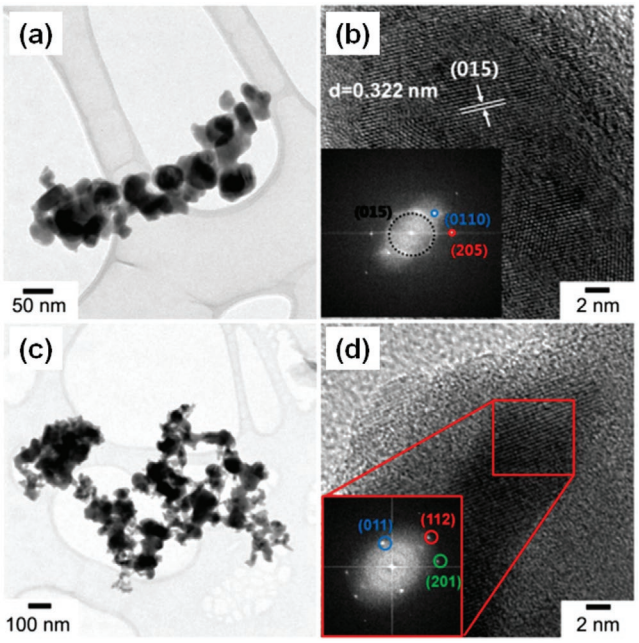

Figure 14. TEM and HR-TEM images as well as FFT patterns of synthesized Bi_2Te_3 a,b) and Te nanopowder c,d) by a chemical reduction process using the used TE module. Reproduced with permission.[140] Copyright 2013, Korean chemical society.

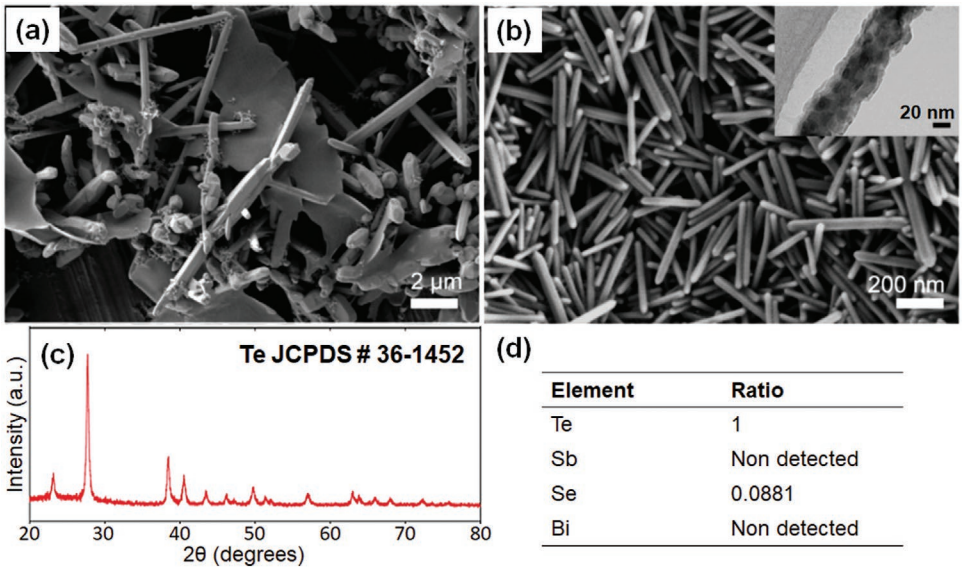

Element	Ratio
Te	1
Sb	Non detected
Se	0.0881
Bi	Non detected

Figure 15. FE-SEM image of sample prepared a) in absence of PVP at pH 13 and b) in the presence of PVP at pH 7 (inset is TEM image of Te nanorods), c) XRD pattern, and d) composition of recycled Te powder. Reproduced with permission.[142] Copyright 2019, Elsevier.

gas-phase tellurium species. Generally, Te solids are considered to be insoluble in aqueous solutions;[148] nonetheless, in presence of EPR3, the soluble ions diffuse across the cell membrane. Inside the cell, two coupled reactions occurred simultaneously (**Figure 16**). The first, which was responsible for the internal bacterial precipitation of metallic tellurium, was a reversible reduction–oxidation reaction between the tellurite ion and metallic tellurium. The other was methylation to a gas-phase tellurium species through the Challenger mechanism, which can diffuse out via the cell membrane and either volatize to the air atmosphere or reform the soluble tellurite ion in the solution.[143]

3.3. Opportunities and Challenges

Considering that the investments in TEGs market are anticipated to increase from 575.9 million US dollars in 2018 to 1713.9 million US dollars by 2027,[149] the simultaneous development of EoL-TE recycling modules is of great importance to pave the way for mass application of TEG products. All three methods reviewed in this section are techno-economically feasible commercial process that can address the economic, energy related, and environmental issues simultaneously. However, all the studies on scarce-element recycling from EoL-TE modules deal with element recycling from modules with simple chemical composition. At present, sustainability is considered as an extra dimension in addition to structure, composition, and morphology when designing new materials.[150] Therefore, with the introduction of new materials such as antimonides, silicides, half heuslers, skutterudites, tetrahedrites, etc., with complex chemical composition, the concurrent development of specified recycling strategies for each established compound is essential. Finally, because of material compositions, industry business models, and recycling-related policies, recycling of scarce elements from EoL-TE modules or devices remains challenging and needs further investigations.

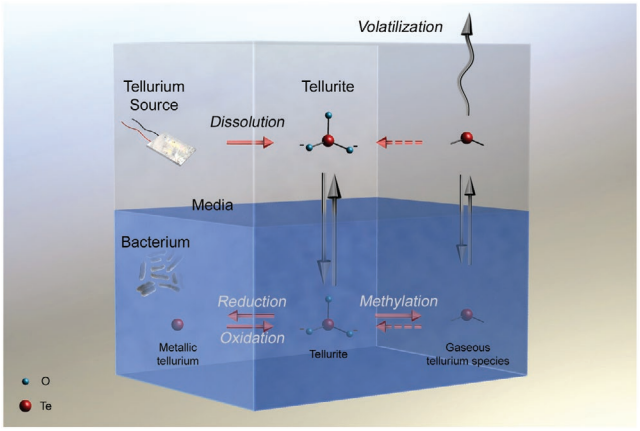

Figure 16. Schematic of tellurium speciation in a bacterium and its media proposed by Bonificio and Clarke.[143] Diffusion is represented by solid arrows, and chemical changes are represented by hollow arrows. Reproduced with permission.[143] Copyright 2014, Society for Applied Microbiology.

4. Summary and Outlook

TE materials can be used for converting waste heat to electricity and for cooling and temperature regulation. For many decades following the development and discovery of new TE materials, not much attention was paid to recycling of this group of materials, mainly because of i) the lack concerns regarding the supply of raw materials, and ii) being far away from the end of TE modules' useful life. During the past couple of decades, as the demand increased, more studies were performed to address the economic and environmental issues associated with the production of new TE materials and disposing of the EoL-TE materials. In this contribution, we have reviewed the progress in using waste materials in the synthesis of TE materials, as well as scarce-element recovery from EoL-TE modules.

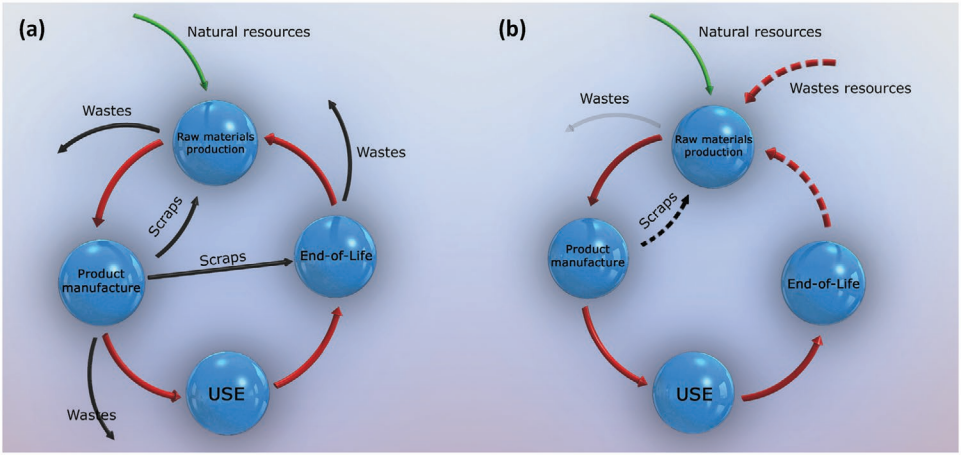

Figure 17. a) A real product life cycle consisting of raw-material production, product manufacture, use and end-of-life stages, and b) modified based on what was done in terms of waste recycling in TE materials. Dashed arrows show the potential areas of developing new strategies in TE waste recycling.

The first use of waste materials in the synthesis of a compound applied as a TE material was in 1993, when SiC was derived from rice husk. Coincidentally, the idea of recycling pure Te or Bi_2Te_3 and PbTe alloys from EoL-TE modules was introduced in the same year. The number of such studies has increased considerably in recent years. For example, the first study on recycling Te from EoL-TE modules was published only in 2013. The newest school of thought on recycling comes from Abol-Fotouh et al.,[151] who used bacteria in environmentally friendly aqueous media to grow large-area bacterial nanocellulose (BC) films with an embedded highly dispersed CNT network. The synthesized thick films possessed low thermal and high electrical conductivity, making them promising as TE modules, which can be wrapped around the heat source and be decomposed enzymatically. Also, So et al.[141] showed that the Te powders recovered from waste TE modules can be used in sensing NO_x gaseous species. The Te paste (Te powder mixed with dimethylformamide (DMF) solvent and ethyl cellulose binder) exhibited a fast reaction rate and a recovery rate of less than three minutes at various gas concentrations. Nevertheless, until full development of fresh ideas that offer environmentally friendly degradation of EoL-TE modules and purposeful and optimized element recovery, the conventional production and synthesis of TE materials will continue, making waste recycling one of the outliers in the TE market.

Figure 17a shows a real product life cycle consisting of raw-material production, product manufacture, use, and end-of-life stages. However, in the case of TE materials, some connecting lines still need to be developed technically and economically to make an efficient and beneficial life cycle (dashed arrows in Figure 17b). Moreover, in order to increase the effectiveness of fabrication of TE modules, discarding the waste from product manufacture to the EoL stage has to be minimized (the line was removed in the modified version). The desirable and profitable strategy is a closed loop in which the end user can take back the used modules to the manufacturer or the raw-material supplier for recycling into refined metals and subsequently new TE modules (Figure 17b). As mentioned in the review, some wastes like rice husk are capable of being used as a source to synthesize Mg_2Si- and SiC-based TE materials. Waste powders and fragments of Bi_2Te_3 and Si, which are the products of manufacturing waste or scrap, can be reprocessed easily for the synthesis of TE materials. And last but not least, it is the recovery of scarce elements such as Te and Se from EoL-TE devices. Each dashed arrow can serve as a new window of opportunity for waste recycling in the field of TE materials.

Considering that all the wastes mentioned in this review and many other potential wastes are produced annually in huge quantities, finding a strategy to return them back to the production cycle is of great importance to meet both industrial and environmental expectations to reduce the final production costs as well as to prevent the degradation of Earth's fragile ecosystems.

Acknowledgements

A.B. acknowledges the Alexander von Humboldt Foundation for the Postdoctoral Research Fellow funding. Special thanks to Ronald Uhlemann for the preparation of the illustrations. The authors acknowledge Prof. Jens Freudenberger for his valuable comments.

Conflict of Interest

The authors declare no conflict of interest.

Keywords

recovery, reutilization, scarce elements, thermoelectric modules, thermoelectric waste materials

Received: December 18, 2019
Revised: February 21, 2020
Published online: March 26, 2020

[1] P. Hutchins, U.S. Energy Information Adminstartion (EIA), https://www.eia.gov/todayinenergy/detail.php?id=39992 (accessed: June 2019).
[2] C. J. Vineis, A. Shakouri, A. Majumdar, M. G. Kanatzidis, *Adv. Mater.* **2010**, *22*, 3970.

[3] T. Torfs, V. Leonov, R. F. Yazicioglu, P. Merken, C. V. Hoof, R. J. M. Vullers, B. Gyselinckx, presented at *SENSORS 2008 IEEE*, Lecce, Italy, Oct **2008**.
[4] Y. Wang, Y. Shi, D. Mei, Z. Chen, *Appl. Energy* **2018**, *215*, 690.
[5] H. Friege, *Waste Manage. Res.* **2012**, *30*, 3.
[6] A. Kumar, M. Holuszko, D. C. R. Espinosa, *Resour., Conserv. Recycl.* **2017**, *122*, 32.
[7] E. Van Eygen, S. De Meester, H. P. Tran, J. Dewulf, *Resour., Conserv. Recycl.* **2016**, *107*, 53.
[8] S. B. Riffat, X. Ma, *Appl. Therm. Eng.* **2003**, *23*, 913.
[9] N. Soltani, A. Bahrami, M. I. Pech-Canul, L. A. González, *Chem. Eng. J.* **2015**, *264*, 899.
[10] A. Bahrami, N. Soltani, M. I. Pech-Canul, C. A. Gutiérrez, *Crit. Rev. Environ. Sci. Technol.* **2016**, *46*, 143.
[11] S. Bose, H. N. Acharya, H. D. Banerjee, *J. Mater. Sci.* **1993**, *28*, 5461.
[12] K. Nielsch, J. Bachmann, J. Kimling, H. Böttner, *Adv. Energy Mater.* **2011**, *1*, 713.
[13] Y. Sun, C.-A. Di, W. Xu, D. Zhu, *Adv. Electron. Mater.* **2019**, *5*, 1800825.
[14] Q. Zhang, Y. Sun, W. Xu, D. Zhu, *Adv. Mater.* **2014**, *26*, 6829.
[15] Y. Zhou, L.-D. Zhao, *Adv. Mater.* **2017**, *29*, 1702676.
[16] J. L. Blackburn, A. J. Ferguson, C. Cho, J. C. Grunlan, *Adv. Mater.* **2018**, *30*, 1704386.
[17] Y. Wang, L. Yang, X.-L. Shi, X. Shi, L. Chen, M. S. Dargusch, J. Zou, Z.-G. Chen, *Adv. Mater.* **2019**, *31*, 1807916.
[18] L. Yang, Z.-G. Chen, M. S. Dargusch, J. Zou, *Adv. Energy Mater.* **2018**, *8*, 1701797.
[19] T. Zhu, Y. Liu, C. Fu, J. P. Heremans, J. G. Snyder, X. Zhao, *Adv. Mater.* **2017**, *29*, 1605884.
[20] S. Jo, S. Choo, F. Kim, S. H. Heo, J. S. Son, *Adv. Mater.* **2019**, *31*, 1804930.
[21] O. Gutfleisch, K. Güth, T. G. Woodcock, L. Schultz, *Adv. Energy Mater.* **2013**, *3*, 151.
[22] S. Zhang, Y. Ding, B. Liu, C.-c. Chang, *Waste Manage.* **2017**, *65*, 113.
[23] A. Işıldar, E. D. van Hullebusch, M. Lenz, G. Du Laing, A. Marra, A. Cesaro, S. Panda, A. Akcil, M. A. Kucuker, K. Kuchta, *J. Hazard. Mater.* **2019**, *362*, 467.
[24] R. G. Morris, R. D. Redin, G. C. Danielson, *Phys. Rev.* **1958**, *109*, 1909.
[25] M. W. Heller, G. C. Danielson, *J. Phys. Chem. Solids* **1962**, *23*, 601.
[26] R. J. LaBotz, D. R. Mason, D. F. O'Kane, *J. Electrochem. Soc.* **1963**, *110*, 127.
[27] R. Chen, *JOM* **2013**, *65*, 702.
[28] T. Iida, Y. Mito, T. Nemoto, *US2010/0051081 A1*, **2010**.
[29] K. Y. Foo, B. H. Hameed, *Adv. Colloid Interface Sci.* **2009**, *152*, 39.
[30] Rice Market Monitor, Vol. XXI, Food and Agriculture Organization of the United Nations (FAO), Rome, Italy **2018**.
[31] G. Cristaldi, A. Latteri, G. Recca, G. Cicala, in Woven Fabric Engineering, Vol. *17* (Ed: P. D. Dubrovski), **2010**, pp. 317–342.
[32] C. Wu, *Sci. News* **2000**, *157*, 164.
[33] M. R. F. Gonçalves, C. P. Bergmann, *Constr. Build. Mater.* **2007**, *21*, 2059.
[34] S. Bose, *Phys. Status Solidi A* **1992**, *129*, 127.
[35] H. N. Acharya, S. K. Dutta, H. D. Banerjee, *Sol. Energy Mater.* **1980**, *3*, 441.
[36] D. M. Rowe, C. Bhandari, *Modern Thermoelectrics*, Holt-Technology, London **1983**.
[37] F. Chigondo, *Silicon* **2018**, *10*, 789.
[38] D. Ginley, M. A. Green, R. Collins, *MRS Bull.* **2008**, *33*, 355.
[39] R. He, W. Heyn, F. Thiel, N. Pérez, C. Damm, D. Pohl, B. Rellinghaus, C. Reimann, M. Beier, J. Friedrich, H. Zhu, Z. Ren, K. Nielsch, G. Schierning, *J. Materiomics* **2019**, *5*, 15.
[40] G. Mesaritis, E. Symeou, A. Delimitis, S. Oikonomidis, M. Jaegle, K. Tarantik, C. Nicolaou, T. Kyratsi, *J. Alloys Compd.* **2019**, *775*, 1036.
[41] L. Lu, M. O. Lai, S. H. Lim, B. W. Chua, C. Yan, L. Ye, *Z. Metallkd.* **2006**, *97*, 169.
[42] Y.-F. Lung, Y.-F. Syu, M.-C. Lin, J.-Y. Uan, *RSC Adv.* **2014**, *4*, 57646.
[43] M. Akasaka, T. Iida, Y. Mito, T. Omori, Y. Oguni, S. Yokoyama, K. Nishio, Y. Takanashi, *MRS Symp. Proc.* **2007**, *1044*, 259.
[44] Y. Honda, T. Iida, T. Sakamoto, S. Sakuragi, Y. Taguchi, Y. Mito, T. Nemoto, T. Nakajima, H. Taguchi, K. Nishio, Y. Takanashi, *MRS Symp. Proc.* **2009**, *1218*, 118.
[45] Y. Isoda, S. Tada, H. Kitagawa, Y. Shinohara, *J. Electron. Mater.* **2016**, *45*, 1772.
[46] J.-I. Tani, H. Kido, *Intermetallics* **2007**, *15*, 1202.
[47] H. Kitagawa, A. Takamoto, S. Imayasu, M. Kitagaki, Y. Isoda, *Mater. Sci. Eng., B* **2018**, *231*, 93.
[48] M. Ioannou, G. Polymeris, E. Hatzikraniotis, A. U. Khan, K. M. Paraskevopoulos, T. Kyratsi, *J. Electron. Mater.* **2013**, *42*, 1827.
[49] G. Mesaritis, E. Symeou, A. Delimitis, M. Constantinou, G. Constantinides, M. Jeagle, K. Tarantik, T. Kyratsi, *J. Alloys Compd.* **2020**, *826*, 153933.
[50] A. U. Khan, N. V. Vlachos, E. Hatzikraniotis, G. S. Polymeris, C. B. Lioutas, E. C. Stefanaki, K. M. Paraskevopoulos, I. Giapintzakis, T. Kyratsi, *Acta Mater.* **2014**, *77*, 43.
[51] Y. Hayatsu, T. Iida, T. Sakamoto, S. Kurosaki, K. Nishio, Y. Kogo, Y. Takanashi, *J. Solid State Chem.* **2012**, *193*, 161.
[52] C. Fanciulli, M. Codecasa, F. Passaretti, D. Vasilevskiy, *J. Electron. Mater.* **2014**, *43*, 2307.
[53] A. U. Khan, N. Vlachos, T. Kyratsi, *Scr. Mater.* **2013**, *69*, 606.
[54] N. Vlachos, G. S. Polymeris, M. Manoli, E. Hatzikraniotis, A. U. Khan, C. B. Lioutas, E. C. Stefanaki, E. Pavlidou, K. M. Paraskevopoulos, J. Giapintzakis, T. Kyratsi, *J. Alloys Compd.* **2017**, *714*, 502.
[55] W. Liu, Q. Zhang, K. Yin, H. Chi, X. Zhou, X. Tang, C. Uher, *J. Solid State Chem.* **2013**, *203*, 333.
[56] R. Inoue, J. Nakano, T. Nakamura, T. Ube, T. Iida, Y. Kogo, *J. Alloys Compd.* **2019**, *775*, 657.
[57] K. Yin, X. Su, Y. Yan, H. Tang, M. G. Kanatzidis, C. Uher, X. Tang, *Scr. Mater.* **2017**, *126*, 1.
[58] N. Farahi, S. Prabhudev, M. Bugnet, G. A. Botton, J. R. Salvador, H. Kleinke, *J. Electron. Mater.* **2016**, *45*, 6052.
[59] H. Alam, S. Ramakrishna, *Nano Energy* **2013**, *2*, 190.
[60] M. Hong, Z.-G. Chen, S. Matsumura, J. Zou, *Nano Energy* **2018**, *50*, 785.
[61] A. I. Boukai, Y. Bunimovich, J. Tahir-Kheli, J.-K. Yu, W. A. Goddard Iii, J. R. Heath, *Nature* **2008**, *451*, 168.
[62] A. I. Hochbaum, R. Chen, R. D. Delgado, W. Liang, E. C. Garnett, M. Najarian, A. Majumdar, P. Yang, *Nature* **2008**, *451*, 163.
[63] C. Chiritescu, D. G. Cahill, N. Nguyen, D. Johnson, A. Bodapati, P. Keblinski, P. Zschack, *Science* **2007**, *315*, 351.
[64] T. C. Harman, P. J. Taylor, M. P. Walsh, B. E. LaForge, *Science* **2002**, *297*, 2229.
[65] X. Ji, B. Zhang, T. M. Tritt, J. W. Kolis, A. Kumbhar, *J. Electron. Mater.* **2007**, *36*, 721.
[66] A. Bahrami, U. Simon, N. Soltani, S. Zavareh, J. Schmidt, M. I. Pech-Canul, A. Gurlo, *Green Chem.* **2017**, *19*, 188.
[67] Z. Bao, M. R. Weatherspoon, S. Shian, Y. Cai, P. D. Graham, S. M. Allan, G. Ahmad, M. B. Dickerson, B. C. Church, Z. Kang, H. W. Abernathy Iii, C. J. Summers, M. Liu, K. H. Sandhage, *Nature* **2007**, *446*, 172.
[68] K. H. Sandhage, M. B. Dickerson, P. M. Huseman, M. A. Caranna, J. D. Clifton, T. A. Bull, T. J. Heibel, W. R. Overton, M. E. A. Schoenwaelder, *Adv. Mater.* **2002**, *14*, 429.
[69] J. R. Szczech, S. Jin, *J. Solid State Chem.* **2008**, *181*, 1565.
[70] F. E. Round, R. M. Crawford, D. G. Mann, *Diatoms: Biology and Morphology of the Genera*, Cambridge University Press, Cambridge **2007**.
[71] H. Bakr, *Asian J. Mater. Sci.* **2010**, *2*, 121.
[72] N. Hayati-Roodbari, R. J. F. Berger, J. Bernardi, S. Kinge, N. Hüsing, M. S. Elsaesser, *Dalton Trans.* **2017**, *46*, 8855.

[73] H. Nakatsugawa, K. Nagasawa, Y. Okamoto, S. Yamaguchi, S. Fukuda, H. Kitagawa, *J. Electron. Mater.* **2009**, *38*, 1387.
[74] M. Fujisawa, T. Hata, H. Kitagawa, P. Bronsveld, Y. Suzuki, K. Hasezaki, Y. Noda, Y. Imamura, *Renewable Energy* **2008**, *33*, 309.
[75] J.-G. Lee, I. B. Cutler, *Am. Ceram. Soc. Bull.* **1975**, *54*, 195.
[76] S. Takeda, C. H. Pai, W. S. Seo, K. Koumoto, H. Yanagida, *J. Ceram. Soc. Jpn.* **1993**, *101*, 814.
[77] P. J. Guichelaar, in *Carbide, Nitride and Boride Materials Synthesis and Processing* (Ed: A. W. Weimer), Springer, Dordrecht, The Netherlands **1997**, pp. 115–129.
[78] D.-M. Liu, B.-W. Lin, *Ceram. Int.* **1996**, *22*, 407.
[79] L. L. Snead, T. Nozawa, Y. Katoh, T.-S. Byun, S. Kondo, D. A. Petti, *J. Nucl. Mater.* **2007**, *371*, 329.
[80] K. Koumoto, M. Shimohigoshi, S. Takeda, H. Yanagida, *J. Mater. Sci. Lett.* **1987**, *6*, 1453.
[81] E. Maeda, M. Komatsu, *The Thermoelectric Performance of Silicon Carbide Semiconductor Made from Rice Hull*, Materials Research Society, Pittsburgh, PA **1996**.
[82] N. A. L. Mansour, S. B. Hanna, *Br. Ceram. Trans. J.* **1979**, *78*, 132.
[83] S. B. Hanna, L. M. Farag, N. A. L. Mansour, *Thermochim. Acta* **1984**, *81*, 77.
[84] E. Maeda, M. Komatsu, E. Tani, H. Tateyama, *J. Ceram. Soc. Jpn.* **2002**, *110*, 804.
[85] D. Radev, I. Uzunov, *Solid State Phenom.* **2010**, *159*, 153.
[86] E. P. Gorzkowski, S. B. Qadri, B. B. Rath, S. K. Singh, presented at The 2011 International Semiconductor Device Research Symposium (ISDRS), MD, December **2011**.
[87] H. J. Goldsmid, R. W. Douglas, *Br. J. Appl. Phys.* **1954**, *5*, 386.
[88] D. M. Rowe, *Thermoelectrics Handbook: Macro to Nano*, CRC Press, Boca Raton, FL **2018**.
[89] I. T. Witting, T. C. Chasapis, F. Ricci, M. Peters, N. A. Heinz, G. Hautier, G. J. Snyder, *Adv. Electron. Mater.* **2019**, *5*, 1800904.
[90] B. Poudel, Q. Hao, Y. Ma, Y. Lan, A. Minnich, B. Yu, X. Yan, D. Wang, A. Muto, D. Vashaee, X. Chen, J. Liu, M. S. Dresselhaus, G. Chen, Z. Ren, *Science* **2008**, *320*, 634.
[91] S. I. Kim, K. H. Lee, H. A. Mun, H. S. Kim, S. W. Hwang, J. W. Roh, D. J. Yang, W. H. Shin, X. S. Li, Y. H. Lee, G. J. Snyder, S. W. Kim, *Science* **2015**, *348*, 109.
[92] M. Gaikwad, D. Shevade, A. Kadam, B. Subham, *Int. J. Curr. Eng. Technol.* **2016**, *4*, 67.
[93] E. M. F. Vieira, J. Figueira, A. L. Pires, J. Grilo, M. F. Silva, A. M. Pereira, L. M. Goncalves, *J. Alloys Compd.* **2019**, *774*, 1102.
[94] *Mineral Commodity Summaries 2019* (Ed.: A. C. Tolcin), U.S. Geological Survey, Reston, VA **2019**.
[95] Z. Su, *Ph.D. Thesis*, Clemson University **2009**.
[96] X. Ji, J. He, Z. Su, N. Gothard, T. M. Tritt, *J. Appl. Phys.* **2008**, *104*, 034907.
[97] Z. Su, J. He, X. Ji, N. Gothard, T. M. Tritt, *Sci. Adv. Mater.* **2011**, *3*, 596.
[98] X. A. Fan, X. Z. Cai, X. W. Han, C. C. Zhang, Z. Z. Rong, F. Yang, G. Q. Li, *J. Solid State Chem.* **2016**, *233*, 186.
[99] Q. Xiang, X. Fan, X. Han, C. Zhang, J. Hu, B. Feng, C. Jiang, G. Li, Y. Li, Z. He, *Mater. Chem. Phys.* **2017**, *201*, 57.
[100] Q. Xiang, X. A. Fan, X. Han, C. Zhang, J. Hu, B. Feng, C. Jiang, G. Li, Y. Li, Z. He, *J. Phys. Chem. Solids* **2017**, *111*, 34.
[101] X. Fan, J. Yang, W. Zhu, S. Bao, X. Duan, C. Xiao, Q. Zhang, Z. Xie, *J. Phys. D: Appl. Phys.* **2006**, *39*, 5069.
[102] J. Yang, T. Aizawa, A. Yamamoto, T. Ohta, *J. Alloys Compd.* **2000**, *309*, 225.
[103] P. K. Guha, M. Siwajek, D. J. Krug, *WO 2017/106243 Al*, **2017**.
[104] V. P. McConnell, *Reinf. Plast.* **2010**, *54*, 33.
[105] Y. Du, J. Xu, B. Paul, P. Eklund, *Appl. Mater. Today* **2018**, *12*, 366.
[106] Q. Meng, Q. Jiang, K. Cai, L. Chen, *Org. Electron.* **2019**, *64*, 79.
[107] Q. Meng, K. Cai, Y. Du, L. Chen, *J. Alloys Compd.* **2019**, *778*, 163.
[108] E. J. X. Pang, S. J. Pickering, A. Chan, K. H. Wong, P. L. Lau, *J. Solid State Chem.* **2012**, *193*, 147.
[109] P. R. Jagadish, M. Khalid, L. P. Li, M. T. Hajibeigy, N. Amin, R. Walvekar, A. Chan, *J. Cleaner Prod.* **2018**, *195*, 1015.
[110] P. R. Jagadish, M. Khalid, N. Amin, L. P. Li, A. Chan, *J. Mater. Sci.* **2017**, *52*, 11467.
[111] P. R. Jagadish, L. P. Li, A. Chan, M. Khalid, *Mater. Manuf. Processes* **2016**, *31*, 1223.
[112] Y. Liu, Q. Wang, J. Pan, Y. Sun, L. Zhang, S. Song, *Chem. - Eur. J.* **2018**, *24*, 9765.
[113] J. J. Ritter, *Inorg. Chem.* **1994**, *33*, 6419.
[114] J. J. Ritter, P. Maruthamuthu, *Inorg. Chem.* **1995**, *34*, 4278.
[115] O. Suominen, V. Mörsky, R. Ritala, M. Vilkko, in *Computer Aided Chemical Engineering*, Vol. *38* (Eds: Z. Kravanja, M. Bogataj) Elsevier, Amsterdam **2016**, pp. 1243–1248.
[116] A. K. Biswas, W. G. Davenport, *Extractive Metallurgy of Copper: International Series on Materials Science and Technology*, Elsevier, Amsterdam **2013**.
[117] H. M. Lee, K. T. Kim, G. H. Ha, *Adv. Powder Technol.* **2011**, *22*, 644.
[118] F. L. B. Mohd Redzuan, M. Ito, M. Takeda, *Intermetallics* **2019**, *108*, 19.
[119] N. Liu, W. A. Jensen, M. Zebarjadi, J. A. Floro, *Mater. Today Phys.* **2018**, *4*, 19.
[120] J. Chai, M. Chen, X. Du, P. Qiu, Y.-Y. Sun, L. Chen, *Phys. Chem. Chem. Phys.* **2019**, *21*, 10497.
[121] D. Leong, M. Harry, K. J. Reeson, K. P. Homewood, *Nature* **1997**, *387*, 686.
[122] A. Laila, M. Nanko, M. Takeda, *Materials* **2014**, *7*, 6304.
[123] A. Laila, M. Nanko, M. Takeda, *Mater. Trans.* **2016**, *57*, 445.
[124] A. Nozariasbmarz, A. Agarwal, Z. A. Coutant, M. J. Hall, J. Liu, R. Liu, A. Malhotra, P. Norouzzadeh, M. C. Öztürk, V. P. Ramesh, Y. Sargolzaeiaval, F. Suarez, D. Vashaee, *Jpn. J. Appl. Phys.* **2017**, *56*, 05DA04.
[125] F. Dąbrowski, Ł. Ciupiński, J. Zdunek, J. Kruszewski, R. Zybała, A. Michalski, K. Jan Kurzydłowski, *Mater. Today: Proc.* **2019**, *8*, 531.
[126] J.-I. Tani, H. Kido, *Jpn. J. Appl. Phys.* **2001**, *40*, 3236.
[127] H. Y. Chen, X. B. Zhao, T. J. Zhu, Y. F. Lu, H. L. Ni, E. Müller, A. Mrotzek, *Intermetallics* **2005**, *13*, 704.
[128] H. Y. Chen, X. B. Zhao, Y. F. Lu, E. Müller, A. Mrotzek, *J. Appl. Phys.* **2003**, *94*, 6621.
[129] X. W. Wang, H. Lee, Y. C. Lan, G. H. Zhu, G. Joshi, D. Z. Wang, J. Yang, A. J. Muto, M. Y. Tang, J. Klatsky, S. Song, M. S. Dresselhaus, G. Chen, Z. F. Ren, *Appl. Phys. Lett.* **2008**, *93*, 193121.
[130] G. Knockaert, presented at *The 12th Int. Conf. on Thermoelectrics*, Yokohama, Japan, November **1993**.
[131] J. D. König, K. Bartholome, H. Böttner, M. K. Altstedde, M. Köhne, J. Nurnus, A. Roch, K. Tarantik, *Thermoelectrics: Power from Waste Heat*, BINE Information Service, Bonn, Germany **2016**.
[132] M. Balva, S. Legeai, L. Garoux, N. Leclerc, E. Meux, *Environ. Technol.* **2017**, *38*, 791.
[133] W. Berger, F.-G. Simon, K. Weimann, E. A. Alsema, *Resour., Conserv. Recycl.* **2010**, *54*, 711.
[134] M. Marwede, A. Reller, *Resour., Conserv. Recycl.* **2012**, *69*, 35.
[135] D. J. Bradwell, S. Osswald, W. Wei, S. A. Barriga, G. Ceder, D. R. Sadoway, *J. Am. Chem. Soc.* **2011**, *133*, 19971.
[136] F. G. Simon, O. Holm, W. Berger, *Waste Manage.* **2013**, *33*, 942.
[137] H. Y. Lee, J. K. Lee, J. G. Jee, J. C. Choi, *US 2014/0112860 A1*, **2014**.
[138] K.-J. Lee, Y.-H. Jin, M.-S. Kong, *J. Nanosci. Nanotechnol.* **2014**, *14*, 7919.
[139] B. Swain, K.-J. Lee, *J. Chem. Technol. Biotechnol.* **2017**, *92*, 614.
[140] D. Kang, *Bull. Korean Chem. Soc.* **2013**, *34*, 2171.
[141] H. So, D.-H. Im, H. Jung, K.-J. Lee, *J. Korean Ceram. Soc.* **2018**, *55*, 90.
[142] H. So, J. Yoo, K. Ryu, M. Yang, K.-J. Lee, *Ceram. Int.* **2019**, *45*, 7226.
[143] W. D. Bonificio, D. R. Clarke, *J. Appl. Microbiol.* **2014**, *117*, 1293.

[144] G. J. Olson, J. A. Brierley, C. L. Brierley, *Appl. Microbiol. Biotechnol.* **2003**, *63*, 249.
[145] T. Rohwerder, T. Gehrke, K. Kinzler, W. Sand, *Appl. Microbiol. Biotechnol.* **2003**, *63*, 239.
[146] B. Volesky, *Hydrometallurgy* **2001**, *59*, 203.
[147] P. Dostálek, in *Microbial Biosorption of Metals* (Eds: P. Kotrba, M. Mackova, T. Macek), Springer, Dordrecht, The Netherlands **2011**, pp. 285–300.
[148] G. K. Schweitzer, L. L. Pesterfield, *The Aqueous Chemistry of the Elements*, Oxford University Press, New York **2010**.
[149] J. Mao, H. Zhu, Z. Ding, Z. Liu, G. A. Gamage, G. Chen, Z. Ren, *Science* **2019**, *365*, 495.
[150] D. Larcher, J. M. Tarascon, *Nat. Chem.* **2015**, *7*, 19.
[151] D. Abol-Fotouh, B. Dörling, O. Zapata-Arteaga, X. Rodríguez-Martínez, A. Gómez, J. S. Reparaz, A. Laromaine, A. Roig, M. Campoy-Quiles, *Energy Environ. Sci.* **2019**, *12*, 716.